Intermediate ocean circulation and cryosphere dynamics in the northeast Atlantic during Heinrich Stadials: benthic foraminiferal assemblage response

Pauline Depuydt, Meryem Mojtahid, Christine Barras, Fatima Zohra Bouhdayad, Samuel Toucanne

Intermediate ocean circulation and cryosphere dynamics in the Northeast Atlantic during Heinrich Stadials: benthic foraminiferal assemblage response

Pauline DEPUYDT[1;*], Meryem MOJTAHID[1], Christine BARRAS[1], Fatima Zohra BOUHDAYAD[1,2], Samuel TOUCANNE[3]

[1] Univ Angers, Nantes Université, Le Mans Université, CNRS, UMR 6112, Laboratoire de Planétologie et Géosciences, F-49000 Angers, France

[2] Presently at: Institute of Geology and Mineralogy, Faculty of Mathematics and Natural Sciences, University of Cologne, Cologne, Germany

[3] Univ Brest, CNRS, Ifremer, Geo-Ocean, F-29280 Plouzane, France

[*] Corresponding author: pauline.depuydt@univ-angers.fr

Abstract

The interaction between ocean circulation and ice-sheet dynamics plays a key role in the Quaternary climate. Compared to the surface and deep compartments of the Atlantic Meridional Overturning Circulation (AMOC), the study of intermediate depths during key time periods, such as Heinrich Stadials (HSs), remains poorly documented, especially in the northeast Atlantic. Here we use benthic foraminiferal assemblage data to trace paleoenvironmental changes from ~32 to 14 ka cal BP at ~1000 m depth in the Bay of Biscay. Our results highlight the high sensitivity of foraminifera, with species-specific responses, to continental (European Ice Sheet dynamics) and marine (AMOC) forcing factors during the last three HSs. In general, HSs were characterized by the concomitant presence of meso-oligotrophic and anoxia indicator species and the low abundance of high-energy indicator species. This confirms an overall sluggish intermediate circulation during the three HSs in the northeast Atlantic. HS1 is distinctive by the abundance of high-organic flux indicator species during its early phase. This is consistent with the fact that HS1 was, by far, the most important period of ice-sheet retreat and meltwater release to the ocean over the studied time interval. Finally, foraminifera depict the mid-HS2 re-ventilation event due to regional glacier instabilities.

Keywords

Intermediate water masses, AMOC, European Ice Sheet, Glacial Eastern Boundary Current (GEBC), Channel River, Benthic foraminifera

1. Introduction

The last glacial-interglacial cycle is a critical period to understand the natural climate variability and its abrupt transitions (*e.g.* Bond *et al.*, 1993; Wang et *al.*, 2001; Clark *et al.*, 2012; Denton *et al.*, 2021). Orbital forcing (solar radiation), and the feedbacks implying the atmosphere, the ocean, and the cryosphere are the main factors explaining the recorded centennial to multi-millennial climate variability over this period (Broecker and Denton, 1990; McManus *et al.*, 1999; Denton *et al.*, 2010; Lynch-Stieglitz, 2017). In the Northern Hemisphere, the climate of the last glacial period was punctuated by cold (stadials) and warm intervals (interstadials), that were coeval with periods of weakened and accelerated Atlantic Meridional Overturning Circulation (AMOC), respectively (*e.g.* Kissel *et al.*, 2008; Böhm *et al.*, 2015; Henry *et al.*, 2016; Toucanne *et al.*, 2021). Amongst the cold intervals, the most drastic are certainly the Heinrich Stadials (HSs), encompassing the Heinrich events (HEs), *i.e.* armadas of icebergs discharge issued from the dislocation of the Hudson Strait Ice stream of the Laurentide Ice Sheet (LIS) that ultimately caused the deposition of ice-rafted debris (IRD) rich sediments in the subpolar North Atlantic (Hemming, 2004). It is hypothesized that HEs were triggered by sub-surface heat (700–1100 m depth), 1-2 ka after the decline of the AMOC (Shaffer *et al.*, 2004; Marcott *et al.*, 2011; Alvarez-Solas *et al.*, 2013). The initial AMOC slowdown likely requires precursor melting of North Atlantic–adjacent ice sheets and it is now accepted that the European Ice sheet (EIS) was a critical source for AMOC destabilization and the initiation of HSs conditions (Peck *et al.*, 2006; Eynaud *et al.*, 2012; Boswell *et al.*, 2019; Toucanne *et al.*, 2015, 2021, 2022).

The present work investigates the evolution of northeast Atlantic intermediate water depth environments and their interaction with EIS dynamics during the last glacial and deglaciation periods, with a focus on HSs. This is achieved through the study of marine sediment core BOBGEO-CS05 retrieved at ~1000 m water depth in the northern Bay of Biscay (BoB) (Figure 1a & 1c). This record covers the past ~32-14 ka cal BP, thus encompassing the last three HSs (HS1, HS2 and HS3). During the last glacial period and the last deglaciation, BOBGEO-CS05 site was located off the Channel River, that drained EIS sediment-laden meltwaters to the northern BoB (Zaragosi *et al.*, 2001; Bourillet and Lericolais, 2003; Toucanne *et al.*, 2009, 2010) (Figure 1b). At the time, the core site was also on the pathway of the Glacial Eastern Boundary Current (GEBC), the glacial analogue of the northward-flowing European Slope Current, that represents the easternmost portion of the upper branch of the AMOC (Toucanne

et al., 2021) (Figure 1b). As such, core BOBGEO-CS05 is ideally located to track EIS melting episodes and evaluate their impact/relation to the upper branch of the AMOC.

The present study focuses on fossil benthic foraminifera as one of the very few biological indicator groups that are able to record the history of events on the seafloor by integrating the cumulative impacts of the changing physico-chemical habitats (*e.g.* Schmiedl and Mackensen, 1997; Wollenburg *et al.*, 2001; Rodriguez-Lazaro *et al.*, 2017). A particular interest is found in documenting HS2 and HS3, which are not covered by the nearby recent foraminiferal studies (Mojtahid *et al.*, 2017; Pascual *et al.*, 2020). In addition, our aim is to establish to what extent information previously obtained from sedimentary, geochemical and surface water proxies on the interaction between the AMOC and the EIS during the HSs are consistent with our benthic biotic data. More specifically, the approach uses here foraminiferal diversity and density, and the ecological requirements of specific species to interpret several aspects of the environment on the seafloor (*e.g.* organic matter flux, bottom-water oxygenation, current, transport, water masses properties). Our findings highlight strong foraminiferal species-specific responses, particularly during HSs, with some species associations able to discriminate between EIS/continental impact and ocean circulation changes.

2. Core location, present and past sedimentological and hydrographical settings

Core BOBGEO-CS05 (46°18.850'N, 5°56.988'W, 1473 cm length, 1015 m water depth) was extracted from the upper continental slope of the northern BoB (northeast Atlantic) during the BOBGEO cruise (doi.org/10.17600/9030060; R/V Pourquoi pas?; Bourillet, 2009) (Figure 1). Core BOBGEO-SC05 is mostly composed of contourite deposits (Toucanne *et al.*, 2021), *i.e.* sediments deposited or substantially reworked by the persistent action (*e.g.* selective deposition, winnowing, erosion) of bottom currents (Facies 1 and 2; Fig. 2). Silty-clayey laminations characterized the early part of the deglaciation (early HS1), ca. 18-16.7 ka (Facies 3; Figure 2), and IRD (Facies 4; Figure 2) allowed the recognition of the Heinrich layers (cf. Supplementary material S1 for the complete X-Ray radiographs).

Today, the sedimentation on the slope is governed by the European Slope Current (ESC), flowing along the upper slope (~500-2000 m water depth) from the northern Iberian Peninsula to the Faroe-Shetland Channel (Marsh *et al.*, 2017; Clark *et al.*, 2021; Moritz *et al.*, 2021) (Figure 1a). This current, driven by both the steep topography of the European margin and

large-scale meridional density gradients (Huthnance, 1984; Pingree and Cann, 1990; Friocourt *et al.*, 2007), is largely recruited from the eastern North Atlantic and is connected, north of ~55°N (*i.e.* Rockall Trough), to the upper part of the North Atlantic Current (NAC; that is the eastern limb of the subpolar gyre). This forms the bulk of the upper branch of the AMOC (down to ~1500 m; Lozier *et al.*, 2019; Huthnance *et al.*, 2020). The latter (to which the ESC contributes by ~25 %; Berx *et al.*, 2013) finally reaches the Nordic Seas convection region, where it cools and sinks to form a deeper southward return flow, the North Atlantic Deep Water (NADW), mainly found along the eastern continental margin of North America and transported by the Deep Western Boundary Current (*e.g.* Dickson and Brown, 1994) (Figure 1a).

The main water mass transported by the NAC into the BoB forms the Eastern North Atlantic Central Water (ENACW), found down to ~600 m water depth (Pollard and Pu, 1985). Below, the Mediterranean Outflow Water (MOW) is present between ~600 and 1500 m, flowing northward from the Gulf of Cadiz and largely entrained by the ESC north of ~45°N (*e.g.* Pingree *et al.*, 1999; van Aken, 2000). Deeper, the Labrador Sea Water (LSW), centered at ~2000 m water depth and corresponding to the upper NADW, dominates (van Aken, 2000a). fcapture of the (southward-flowing) LSW by the above (eastward-flowing) Gulf Stream – NAC system in the north-western North Atlantic (Buckley and Marshall, 2016; Zou *et al.*, 2017) (Figure 1a).

During the last glacial maximum (LGM) ca. 23-18 ka cal BP (Mix *et al.*, 2001), the Gulf Steam – NAC system and more generally the upper branch of the AMOC certainly had a different geometry (*i.e.* positioned southward) because of the (southward) expansion of ice sheets over North America (Keffer *et al.*, 1988; Otto-Bliesner *et al.*, 2006; Brady and Otto-Bliesner, 2011; Löfverström *et al.*, 2014) (Figure 1b). The NADW was likely replaced by a shallower, northern-sourced nutrient-poor water mass, namely the Glacial North Atlantic Intermediate Water (GNAIW), dominant above 2000 m depth and overlaying a more nutrient-rich water of southern origin below 2000 m (*i.e.* a glacial analog of Antarctic Bottom Water) (*e.g.* Lynch-Stieglitz *et al.*, 2007). The recirculation of the GNAIW by the glacial Gulf Stream – NAC system certainly explains GNAIW signatures recorded in the NE Atlantic basin and the BoB basin during the last glacial period (Zahn et al., 1997; Peck et al., 2006, 2007a; Toucanne et al., 2021). At the same time, the Mediterranean-Atlantic water exchange was reduced by ~50 %, and the MOW was certainly restricted to the southern Iberian margin (*e.g.* Rogerson *et al.*, 2012). On the other hand, the presence of Antarctic Intermediate waters (AAIW) along the European margin as far north as the South Iceland Rise was hypothesized (Rickaby and Elderfield, 2005; Thornalley *et al.*, 2010) but the recent studies of Thornalley *et al.* (2015) then

Crocker *et al.* (2016) concluded that mid-depth in the NE Atlantic was never ventilated by southern-sourced waters during the last glacial period. During late HS1 (~17 ka cal BP), and the near shutdown of the AMOC (McManus *et al.*, 2004; Ng *et al.*, 2018), Mojtahid *et al.* (2017) recorded low foraminiferal Sr/Ca ratios (*i.e.* carbonate system proxy; Yu *et al.*, 2014; Allen *et al.*, 2016; Keul *et al.*, 2017), indicative of a change in water mass chemistry and origin in the BoB. At the same time, Mojtahid *et al.* (2017) recorded increasing benthic foraminiferal Mg/Ca ratios, indicating a warming of intermediate water masses. This is interpreted as the northward conveyance of the subsurface warming originating from the low latitudes (Rühlemann *et al.*, 2004; Shaffer *et al.*, 2004) by the glacial NAC (GNAC) and the GEBC (Figure 1b) (Toucanne *et al.*, 2021). This reinforces the view that the water mass structure in the glacial NE Atlantic could have changed rapidly through time.

3. Materials and Methods

3.1. Chronology

The chronostratigraphic framework of core BOBGEO-CS05 (Figure 2) is detailed in Toucanne *et al.* (2021). In short, the final age model is based on XRF-Ca/Ti data synchronization with the nearby well-dated core MD95-2002 (Figure 2a). Twenty-one XRF tie-points based on the recognition of millennial-scale oscillations were determined. The final age model indicates that core BOBGEO-CS05 covers a period extending from ca. 32 to 14 ka cal BP (Figure 2), thus encompassing the end of MIS 3 (ca. 57-29 ka cal BP) and MIS 2 (ca. 29-14.7 ka cal BP). The accuracy of the age model is supported first by the good match between the percentages of the polar planktonic taxon *N. pachyderma* in core BOBGEO-CS05 and MD95-2002 (Figure 2c), and second, by the overall concordance with the new radiocarbon dates (n=12; Table 1; Figure 2b). The top core ^{14}C dates show older ages (~15.7 cal ka BP) than the final XRF-Ca/Ti based age model (~14 cal ka BP) (Figure 2b). The low percentages of the polar taxon *N. pachyderma* at the core top (Figure 2c) indicate that we are out of the Heinrich Stadial, making the core top ^{14}C ages unreliable. Such incoherencies in ^{14}C dates (including the few outliers; Figure 2b) are certainly linked to physical sediment mixing and bioturbation that are common in contourite deposits.

The final age model clearly shows a sedimentary hiatus after ~14 cal ka BP, in concordance with previous studies in similar environments in the BoB (Mojtahid et al., 2017; Toucanne et al., 2021). The lack of sedimentation is due to increased erosion of the shelf deposits in response

to the significant sea-level rise and the embayment of the English Channel (e.g., Bourillet *et al.*, 2003; Toucanne *et al.*, 2012).

Core BOBGEO-CS05 shows sedimentation rates of 50-150 cm.ka^{-1} (Figure 2b). As such, core BOBGEO-CS05 offers a unique opportunity to study at high time resolution the later part of the last glacial period and the last three HSs.

3.2. Foraminiferal analyses

For benthic foraminiferal analyses, 56 samples were investigated (~320 years resolution). The samples were washed through 63 and 150 µm mesh size sieves. The >150 µm fraction was splitted with a dry Otto microsplitter (when necessary) until obtaining at least 250-300 specimens in the final split. Then, all foraminifera were picked out from the split and mounted on Plummer cell slides for taxonomic determination. To verify the relevance of small-sized benthic species, 16 out of the 56 samples were investigated from the 63-150 µm size fraction. Foraminifera were picked out from 3 out of the 16 samples, put in Plummer cell slides and determined taxonomically. For the rest of the 63-150 µm samples, foraminifera were counted and determined directly under the stereomicroscope. Similarly to the >150 µm fraction, samples (63-150 µm) were splitted with a dry Otto microsplitter until obtaining at least 250-300 specimens in the final split. The benthic foraminiferal accumulation rate (ind.cm^{-2}.ka^{-1}) (BFAR), used as paleo-productivity proxy (Herguera and Berger, 1991; Herguera, 1992; Gooday, 2003; Jorissen *et al.*, 2007), was calculated for both the >150 µm and >63 µm (63-150 + >150 µm) fractions as: number of individuals per gram of dry sediment × linear sedimentation rate (cm.ka^{-1}) × Dry Bulk Density (g.cm^{-3}) (Herguera and Berger, 1991). The Dry Bulk Density (DBD) was calculated following the relation: $DBD = 2.65 \times (1.024 - D_{wet})/(1.024-2.65)$, where 2.65 g.cm^{-3} is the grain density and 1.024 g.cm^{-3} is the interstitial water density (Auffret *et al.*, 2002). Wet bulk densities (D_{wet}) were derived from gamma-ray attenuation density measurements obtained from a 'Geotek Multi Sensor Core Logger' (MSCL).

The relative abundances of benthic species (% of the total foraminiferal abundances) were calculated for the >150 µm fraction for the 56 samples and for the >63 µm fraction (63-150 µm + >150 µm) for the selected 16 samples. The error bars of the relative abundances were computed with the binomial standard error $\sqrt{(p(1-p))/n}$ (Buzas, 1990; Fatela and Taborda, 2002), where p is the species proportion estimate (number of counted individuals for a given species/n). The diversity of the 56 samples (>150 µm) was calculated with the Shannon index (entropy, H; Hayek and Buzas, 1997) using the PAST software (PAleontological STatistics;

Version 2.14; Hammer *et al.*, 2001). Error bars representing 95 % confidence interval were computed with a bootstrap procedure. In this study, we discuss mainly the most dominant species with relative abundance >10 % showing the highest variability. All species with relative abundance between 5 and 10 % in at least one sample are presented in supplementary material S2, and their ecological interpretations summarized in Table 2. The complete raw data set is available as supplementary material S3 and in SEANOE data repository (https://doi.org/10.17882/88029). Scanning Electron Microscope (SEM) photographs were obtained at LPG (Angers University, France) using a Tabletop Microscope Hitachi TM4000Plus.

For the counts of the planktonic taxon *N. pachyderma*, the >150 µm fraction were used and the relative abundances were determined using a minimum of 300 planktonic foraminiferal tests from single sample splits. Counting was performed at University of Bordeaux (France).

4. Results

Average BFAR values from the >150 µm fraction are ~12.10^3 ind.cm^{-2}.ka^{-1} and from the >63 µm are ~$7.5.10^6$ ind.cm^{-2}.ka^{-1} (Figure 3a). The values from the >150 µm fraction are minimal during the three HSs (~1.10^3 ind.cm^{-2}.ka^{-1}) and are more important during the interstadial periods (~30.10^3 ind.cm^{-2}.ka^{-1}). From ~32 to 14 ka cal BP, the Shannon (H) index (Figure 3b) shows an overall increase of diversity, with values ranging from ~2 to 3.2.

The eight most dominant species (>10 %) showing the highest variability are illustrated in Plate 1 and their relative abundances are presented in Figure 3 (c-j). *Elphidium* spp., *Cassidulina crassa* and *Cibicides lobatulus* are dominant along the record and account together for 12.7 to 74.3 % of the total fauna. In this study, *Elphidium* spp. includes mainly *E. excavatum* (*i.e. E. excavatum* f. *clavatum*) with pyritized shells (Plate 2a) and other species of the genus *Elphidium* (e.g., *E. gerthi*, *E. macellum*). *Elphidium* spp. show maximum values (>30 %) between 30.7 and 28.9 ka cal BP (*i.e.* HS3) and minimum values (<10 %) between 17.5 and 16.5 ka cal BP (*i.e.* Early HS1; Figure 3c). Before HS2, *C. crassa* accounts in average for about ~21 % of the total fauna (Figure 3d). The highest values are recorded during HS2, with maximum percentages (40 %) just before HE2 followed by a sharp decrease. After HS2, the relative density of this species remains stable around ~8 %. *Cibicides lobatulus* exhibits a different pattern in comparison with the previously mentioned species. Generally, this species is present with lower proportions during HS periods (around 5-10 %), except at 24.2 ka cal BP

(during HE2) and 17.2 ka cal BP (during HS1). Between HS3 and HS2 (ca. 29-26 ka cal BP) and during the LGM (ca. 23-18 ka cal BP), *C. lobatulus* accounts for ~22 % of the total fauna (Figure 3e). *Trifarina angulosa* shows the same trend as *C. lobatulus* (Figure 3f) but with overall lower proportions (maximum values around 10 %). The remaining dominant species (>10 %) present a discontinuous evolution. *Cassidulina carinata*, *Bolivina* spp. and *Globobulimina* spp. exhibit high relative abundances (up to 42 %, 24 % and 18 % respectively), with high variability, during early HS1 (Figure 3g, 3h & 3i). Before HS1, *Globobulimina* species are almost absent except in samples from HS3 and HS2 (average of ~5 % and 7.5 %, respectively). *Cibicidoides pachyderma* is also present mainly during the three HSs reaching 12.5 % at 29.3 ka cal BP (*i.e.* during HS3), 20 % at 25.3 ka cal BP (*i.e.* during HS2) and varying around 10 % at ~HS1 (Figure 3j). Here, *C. pachyderma* encompasses several morphotypes spanning from *C. pachyderma* sensu stricto (pronounced carina) to *Cibicidoides kullenbergi* sensu stricto (less pronounced carina) (Plate 2b). The presence of several intermediate morphotypes hampered the taxonomical differentiation between *C. pachyderma* and *C. kullenbergi*, and as such were lumped together as *C. pachyderma.*

The evolution through time of the minor species (*i.e.* present only few times with percentages >5 %) is represented in **Erreur ! Source du renvoi introuvable.**. *Gavelinopsis praegeri* and *Planorbulina mediterranensis* mainly appear just after 24.2 ka cal BP, between HE2 and the end of HS2. *Chilostomella oolina*, *Pullenia quinqueloba*, *Textularia sagittula* occur just one time with relative densities >5 % at 16.8 ka cal BP, 16.5 ka cal BP, 17.2 ka cal BP respectively while *Hoeglundina elegans* occurs only at 14 ka cal BP. *Nonionella turgida* become dominant only after HE1 (~6 %).

In the small fraction (63-150 µm), the identified species were similar to the ones found in the larger size fraction (>150 µm). When considering the small and large fractions together (>63 µm), six major species >5 % are present: *Elphidium* spp., *C. crassa*, *C. lobatulus*, *C. carinata*, *Bolivina* spp. and *T. angulosa.* These species, also identified as major species when considering only the >150 µm size fraction, exhibit approximately similar trends (black dashed line; Fig. 3 c-h). Only *C. crassa* presents much higher proportions in the >63 µm fraction with abundances ranging from 15 to 60 % of the total fauna.

5. Discussion

5.1. Regional inter-comparison of benthic foraminiferal faunas

Most of the dominant foraminiferal taxa in core BOBGEO-CS05 (*e.g. C. pachyderma*, *C. carinata*, *C. crassa*, *Bolivina* spp., *Globobulimina* spp.) inhabit the modern upper slope environments of the BoB (*e.g.* Murray, 1970; Fontanier *et al.*, 2006; Mojtahid *et al.*, 2010; Duros *et al.*, 2011, 2012; Dorst and Schönfeld, 2013), and/or are found in the regional benthic fossil (*i.e.* last glacial) records of intermediate waters depths (Figure 1c; Mojtahid *et al.*, 2017; Pascual *et al.*, 2020). However, some discrepancies are observed and detailed hereafter:

5.1.1. High-energy indicator species

Cibicides lobatulus (also known as *Lobatula lobatula*) is highly dominant in our record (~4-30 %). This species is also present, but with overall lower percentages (~10 %), at site MD99-2328, north of our study site (Figure 1), that covers the time interval from 23 to 16 ka cal BP (Mojtahid *et al.*, 2017) (Figure 3). However, this epibenthic species is absent today from the BoB modern foraminiferal communities at ~1000 m depth (*e.g.* Fontanier *et al.*, 2002; Fontanier *et al.*, 2006; Mojtahid *et al.*, 2010; Duros *et al.*, 2011, 2012). This discrepancy can be explained by different environmental conditions (*e.g.* food source, hydrodynamics) during the last glacial period allowing their settlement at intermediate water depths in the area. Indeed, *C. lobatulus* is a suspension-feeder that inhabits moderate-to-strong hydrodynamic environments of the modern northeast Atlantic. These include shelf environments (*e.g.* Basque shelf; Pascual *et al.*, 2008) and upper slope settings swept by strong bottom currents and characterized by coarse substrate and/or cold-water coral mounds and reefs trapping abundant food particles (*e.g.* Gulf of Cadiz, Porcupine and Rockall Banks; Schönfeld, 1997, 2002a, 2002b; Margreth *et al.*, 2009; Spezzaferri *et al.*, 2015). As such, the high presence of *C. lobatulus* in the BOBGEO-CS05 glacial record might indicate stronger currents than today. The depicted link between *C. lobatulus* and strong energy environments is further supported in our record by its co-variation with: i) the abundance of *Trifarina angulosa* ($r^2 = 0.78$) (Figure 3e & 3f) which is commonly associated with shelf-edge to upper-slope areas swept by vigorous bottom currents (*e.g.* southwest Norway, Rockall Trough ; Mackensen et al., 1985; Austin and Evans, 2000; Gooday and Hughes, 2002), and ii) the "sortable silt" mean size $\overline{SS}$ (*i.e.* the mean grain size of the carbonate-free terrigenous silt fraction) at BOBGEO-CS05 (Figure 4f; Toucanne *et al.*, 2021) that provides a direct constraint on the rate of past bottom flows (McCave *et al.*, 1995). As such, our biotic data independently support the presence of strong bottom currents on the upper slope

of the BoB, and by extent the presence of the GEBC along the French Atlantic margin (Toucanne *et al.*, 2021). Based on the above, we summed the percentages of *C. lobatulus* and *T. angulosa* to constitute the group of high-energy indicator species. The latter will be used to examine the hydrodynamics variability in the study area throughout the ca. 32-14 ka cal BP interval, and more specifically during the HSs (cf. Section 5.2).

5.1.2. Glacier-proximal species

The high dominance (up to ~40 % in the late MIS 3 and ~20 % thereafter) of elphidiids in core BOBGEO-CS05 is peculiar as this group is presently found in coastal, shelf and estuarine environments of the northeast Atlantic (*e.g.* Pujos, 1976; Murray, 2014; Mojtahid *et al.*, 2016). In the modern benthic foraminiferal assemblage of the upper Whittard region (northern BoB, ~1000 m depth; Duros *et al.*, 2012), *Elphidium* spp. are found only in the dead faunas, and as such, were considered as transported from shallower settings. Mojtahid *et al.* (2017) report high abundances of *Elphidium* spp. in core MD99-2328 especially during the late HS1 (16.7-16 ka cal BP; up to ~70 %) and hypothesized their transport to these intermediate depths by the EIS icebergs and/or shelf ice. This would be also a possibility for BOBGEO-CS05 since *Elphidium* shells show pyritization marks (Plate 2a) that may indicate a potential reworking and transport. However, it is interesting to note that modern elphidiids may extend their habitats to deeper settings (several hundred meters) in cold, arctic environments, usually in connection with freshwater river outflow (*e.g.* Bergsten, 1994; Polyak *et al.*, 2002). Therefore, another explanation for the high abundance of elphidiids in the glacial BOBGEO-CS05 record could simply be an adaptation to cold glacial conditions and meltwater inputs in the BoB. This is supported by the presence of *E. excavatum* f. *clavatum*, the dominant elphidiids species in our assemblages (~75 %), frequently found today in glacier-proximal environments (*e.g.* Jennings *et al.*, 2004; Murray, 2006; Darling *et al.*, 2016; Fossile *et al.*, 2020). The modern conditions in the polar regions where this species lives today are close to the conditions prevailing during the last glacial period in our study area since the EIS invaded the western European shelf (cf. ice-sheet and polar fronts limits in Figure 1) and the Channel River channeled huge amounts of meltwaters to the northern BoB.

Cassidulina crassa occurs concomitantly to *E. excavatum* f. *clavatum* in our record (r^2 = 0.85). Similarly to *Elphidium* spp., modern upper slope foraminiferal studies from the BoB reported that *C. crassa* is either only encountered in the dead faunas or very rarely present in

the living faunas (*e.g.* Fontanier *et al.,* 2002 , 2006; Mojtahid *et al.,* 2010; Duros *et al.,* 2012). It is therefore probable that this species has been transported to the study site, although *C. crassa* tests are rather intact (Plate 1) compared to *E. excavatum* f. *clavatum* (Plate 2a). It must be noted that the morphospecies identified here as *C. crassa* (d'Orbigny, 1839) has a variant that is very close morphologically and was described first as *Cassidulina crassa* var. *reniforme* Nørvang, 1945, and later elevated to the species rank as *C. reniforme*. *Cassidulina reniforme* morphospecies is mainly reported from arctic regions as typical of near-glacier environments (Hansen and Knudsen, 1995; Korsun *et al.,* 1995; Murray, 2006). Thus, it is highly possible that *C. crassa* from BOBGEO-CS05 is actually the same morphospecies than the one reported from arctic regions. We therefore assume that the *C. crassa* - *E. excavatum* f. *clavatum* association in our record is coherent with near-glacier environments. This is further corroborated by the absence of these species in the upper slope glacial record PP10-12 from the southeast BoB (Pascual *et al.,* 2020), far from both the ice sheet extent limit and the Channel River mouth. Based on the above, we summed the percentages of *E. excavatum* f. *clavatum* and *C. crassa* to constitute the group of glacier-proximal indicator species. The latter will be used to examine the EIS dynamics (cf. Section 5.2).

5.1.3. Holocene indicator species

One of the most striking features of our benthic foraminiferal record is the absence of uvigerinids (*e.g. U. peregrina, U. mediterranea*), whereas they dominate the modern benthic foraminiferal assemblages of the BoB between ~500 and 2000 m water depth (e.g., Schönfeld, 2006; Barras *et al.,* 2010; Mojtahid *et al.,* 2010; Duros *et al.,* 2011, 2012). This absence is also the case in the glacial part of the MD99-2328 record (Mojtahid *et al.,* 2017). We assume therefore that uvigerinids might not be tolerant to the glacial-related conditions on the BoB seafloor (Mojtahid *et al.,* 2013; Pascual *et al.,* 2020; Rodriguez-Lazaro *et al.,* 2017). Schönfeld and Altenbach (2005) hypothesized a widespread change from glacial to modern surface productivity configuration (*e.g.* nature of primary producers, seasonality in phytoplankton blooms) that may have triggered the Holocene settlement of *U. peregrina* in the northeast Atlantic. It is also interesting to note that *U. peregrina* and *U. mediterranea* are very abundant in bathyal depths (~200-1500 m) of the Mediterranean and the BoB bathed by the MOW (*e.g.* De Rijk *et al.,* 2000; Schmiedl *et al.,* 2000; Fontanier et al., 2003). The possible link between water masses and specific fauna has been progressively abandoned in favor of organic matter and oxygen as major controlling environmental parameters (Jorissen *et al.,* 2007). Yet, the

settlement of uvigerinids in the BoB in the end of deglaciation - early Holocene (Garcia *et al.*, 2013; Mojtahid *et al.*, 2013; Pascual *et al.*, 2020) seems to coincide with the significant increase in the influx of the MOW into the North Atlantic and along the European margin (Rogerson *et al.*, 2012; Lebreiro *et al.*, 2018). This is coherent with what Mojtahid *et al.* (2017) observed in core MD99-2328 where they record the appearance of uvigerinids (although with low abundances) only in the Holocene portion of the record.

In summary, we have shown that the upper slope benthic foraminifera assemblage found at site BOBGEO-CS05 reflect the complex, highly dynamic and variable environmental conditions in the northern BoB during the last glacial period, including high bottom water currents, glacier-proximal settings, and southern retreat of the MOW. Since benthic foraminifera respond greatly to these various environmental parameters, they present a great potential to better constrain glacial intermediate bottom water characteristics during HSs.

5.2. Environmental particularities of Heinrich Stadials depicted by benthic foraminifera

5.2.1. What do the last three Heinrich Stadials have in common in the Bay of Biscay?

In general, HS3 (~31-29 ka cal BP), HS2 (~26-23 ka cal BP) and HS1 (~18-15.5 ka cal BP) in core BOBGEO-CS05 are characterized by a systematic drop in BFAR values (Fig. 3a). This may indicate unfavorable conditions (*e.g.* low quality/quantity of the organic matter, low oxygenation) for the growth and reproduction of foraminifera. In the same intervals, we record the highest occurrence of *Cibicidoides pachyderma* and *Globobulimina* spp. (Figure 3j & 3i). C*ibicidoides pachyderma* is usually found in meso-oligotrophic open-slope environments, as in the modern BoB (Schmiedl *et al.*, 2000; Mojtahid *et al.*, 2010; Duros *et al.*, 2012). *Globobulimina* spp., on the other hand, are deep infaunal species that tolerate hypoxia and anoxia (Risgaard-Petersen *et al.*, 2006; Pina-Ochoa *et al.*, 2010; Koho *et al.*, 2011). Hence, we interpret the *C. pachyderma* - *Globobulimina* spp. association (*i.e.* meso-oligotrophic species; see Figure 4h) during HSs, together with the low BFAR, as indicating meso-oligotrophic conditions, with moderate to low export of organic matter to the seafloor, and reduced bottom-water ventilation. The latter is supported by the concomitant decrease in the proportions of high-energy indicator species *T. angulosa* and *C. lobatulus* during each of the HSs (Figure 4g). The weak hydrodynamics during the HSs is independently supported by the low $\overline{SS}$ values at

BOBGEO-CS05 and at many sites along the French Atlantic margin (Toucanne *et al.*, 2021). As such, biotic and sedimentological data indicate reduced near-bottom flow speed (*i.e.* weakened GEBC) and, by extension, a sluggish AMOC during the three HSs.

The glacier-proximal species (*E. excavatum* f. *clavatum*. and *C. crassa*), although present all along the BOBGEO-CS05 record, display the highest percentages during the HSs, especially during HS3 and HS2 (Figure 4b). In their modern habitats in the Arctic fjords, these species are impacted by seasonal melting of marine-terminating glaciers (Schroder-Adams *et al.,* 1990; Wollenburg and Mackensen, 1998; Wollenburg and Kuhnt, 2000; Wollenburg *et al.,* 2004). Since enhanced EIS meltwaters influx to the BoB are described during HSs (Toucanne *et al.,* 2015), increased densities of these species might be indicative of such meltwater inputs. The concomitant presence of meso-oligotrophic species (*e.g. C. pachyderma*) indicates a low to moderate export of organic matter to the seafloor, especially during HS2 and HS3. This will be further discussed when addressing the specificities of each HS (cf. Sections 5.2.2. and 5.3).

5.2.2. The difference between the early HS1 and the other HSs

In core BOBGEO-CS05, HS1 is very distinct from HS2 and HS3 by displaying a high presence (~60 %) of opportunistic and high-organic flux indicator species (*C. carinata* and *Bolivina* spp.; Schmiedl *et al.,* 1997; Fontanier *et al.,* 2003; Duros *et al.,* 2011) during its early phase ca. ~18-16.7 ka cal BP (Figure 4d). This is coherent with the findings of Mojtahid *et al.* (2017) at the same time period at site MD99-2328. Conversely, during HS2 and HS3, these species were present with much lower abundances (< 10 %; Figure 4d). Thus, we assume that limited organic material inputs reached the BOBGEO-CS05 site during HS3 and HS2, then substantially increased during the early HS1. This difference is further corroborated by the positive correlation between the abundance of the high-organic flux indicator species during early HS1 at our site and both the BIT index at site MD95-2002 (Figure 4c; Ménot *et al.,* 2006) and the turbidite (*i.e.* flood-related deposits) flux in the deep BoB (Zaragosi *et al.,* 2006; Toucanne *et al.,* 2008, 2012). It has been suggested that these differences in organic material inputs through time could result from complex interactions between climate conditions, and ice and vegetation cover (Ménot *et al.,* 2006). Our data cannot resolve this issue, but it certainly highlights the paroxysmal phase of EIS melting in response to increasing boreal insolation during HS1, and the concomitant rapid progradation of a large outer-shelf delta that ultimately improved the connection between the BOBGEO-CS05 site and the Channel River system (Toucanne *et al.,* 2012). That said, because *C. carinata* and *Bolivina* spp. are very abundant in

shallower settings in the BoB (140-550 m depth; Duros *et al.*, 2011 ; Fontanier *et al.*, 2003), we cannot discard that their presence in our record is a result of downslope transport. Even so, the abundance of these species still indicates increased organic fluxes in their source habitats.

Interestingly, in the upper slope BOBGEO-CS05 and MD99-2328 cores, the dominance of the anoxia indicator species (representing the sum of *Globobulimina* spp. and *Chilostomella oolina*) at HS1 occurs early within this interval, before HE1 event *sensu stricto* (Figure 4i). According to Mojtahid *et al.* (2017), the presence of these indicator species during early HS1 is indicative of organically-enriched and/or oxygen-depleted benthic environments, and their absence during HE1 event, together with high $\overline{SS}$ (Figure 4i & 4f) indicate well-ventilated intermediate waters. In deeper sediment cores from the BoB (>2000 m depth), the HE1 event is characterized by the presence of authigenic carbonates indicating anoxic bottom waters (*e.g.* Auffret *et al.*, 1996; Toucanne *et al.*, 2015). Because these anoxia markers are not observed in the shallower cores BOBGEO-CS05 and MD99-2328 and because all proxies ($\overline{SS}$ and foraminifera; Figure 4) indicate well-ventilated bottom waters, we can hypothesize a decoupling between a vigorous intermediate water depth circulation during HE1 and a still sluggish circulation at >2000 m in the northeast Atlantic, as reported by the Bermuda rise $^{231}Pa/^{230}Th$ data from the deep northwest Atlantic (Figure 4e). A similar pattern is found in the equatorial Atlantic where a better ventilation of mid-depth waters in late HS1 is recorded while the deep sites remained poorly ventilated (Chen *et al.*, 2015).

5.3. Foraminiferal evidence for mid-HS2 re-ventilation event

During HS2 (Figure 5), the overall meso-oligotrophic conditions and the low bottom-water ventilation depicted by both the low BFAR and the *C. pachyderma* - *Globobulimina* spp. association (*i.e.* meso-oligotrophic species) were interrupted around 24.3 ka cal BP (Figure 5d & 5e). At the same time, low percentages of the polar planktonic species *N. pachyderma* (Figure 5a) indicate a a warming of the sea-surface conditions and therefore a cessation of meltwater input in the northern BoB. This surface water warming is recorded in several sedimentary records along the European margin (*e.g.* Scourse *et al.*, 2009; Austin *et al.*, 2012; Waelbroeck et al., 2019). This warm event interrupting HS2 seems to be coeval with a well-known atmospheric decrease in dust flux at high latitudes (Rasmussen *et al.*, 2008; Austin *et al.*, 2012). During this sea-surface warming event, the re-appearance of the high-energy indicator species (Figure 5c) and the drop in the anoxia indicator species (Figure 5f) strongly suggests a

456 reactivation of bottom water currents at site BOBGEO-CS05. This is supported by the increase
457 in the $\overline{SS}$ values at our site and, more generally, in the northern part of the French Atlantic
458 margin (Figure 5b). Our biotic data, although covering this millennial-scale event at low
459 sampling resolution, thus indicate, together with the $\overline{SS}$ proxy, enhanced vigor of the GEBC
460 and, by extension, of the AMOC during the mid-HS2. This re-acceleration of the GEBC
461 continues to about100 yrs before the iceberg debacle of the LIS (*i.e.* HE2 *sensu stricto* at
462 24.2 ka cal BP), when our biotic and sedimentological proxies show a rapid return to meso-
463 oligotrophic conditions at the sea-floor and weak bottom currents.

464

465 ## 6. Conclusions

466 Benthic foraminiferal assemblage data allowed us to reconstruct the paleoenvironmental
467 evolution of the upper slope of the BoB (site BOBGEO-CS05) over the ca. 32-14 ka cal BP
468 period. In general, species-specific responses reflect the complex, highly dynamic and variable
469 environmental conditions in the northern BoB during the last glacial period, including
470 fluctuations in the bottom water current and the GEBC, changes in organic matter fluxes and
471 Channel River discharges, and latitudinal changes of the MOW.

472 The three HSs (HS3, HS2 and HS1) present some common features. They are all
473 characterized by an overall low proportion of high-energy indicator species (*i.e. Cibicides*
474 *lobatulus* and *Trifarina angulosa*), and a significant presence of meso-oligotrophic indicator
475 species (*Cibicidoides pachyderma*), anoxia indicator species (*Globobulimina* spp. and *C.*
476 *oolina*), and glacier-proximal species (*E. excavatum* f. *clavatum* and *Cassidulina crassa*). In
477 agreement with previously published sedimentological and geochemical proxies, this reflects
478 overall low organic matter fluxes to the seafloor and a low bottom water ventilation during the
479 HSs.

480 Detailed investigation of the benthic foraminifera reveals some specificities of the HSs in
481 the northeast Atlantic. First, the high abundance of high-organic flux indicator species
482 (*Cassidulina carinata* and *Bolivina* spp.) during early HS1, compared to their near absence
483 during HS2 and HS3, reveals a millennial-scale peak in terrestrial organic material in the BoB
484 resulting from the significant EIS melting and Channel River meltwater floods. Second, benthic
485 foraminiferal species depict a short-term mid-depth re-ventilation event during HS2, indicated
486 by a decrease in the proportions of anoxia indicator species and an increase in the abundance
487 of high-energy indicator species. This short-term reactivation of the GEBC along the French

Atlantic margin, and of the AMOC, is coherent with the cessation of the EIS meltwater input in the northern BoB, and more generally, with a warming of the sea-surface conditions in the northeast Atlantic. This result strongly emphasizes the connection between the intermediate ocean circulation and the cryosphere dynamics in the northeast Atlantic during the Heinrich Stadials.

7. Acknowledgments

This study was funded by the CNRS-INSU-LEFE-IMAGO program (STING project), the ARTEMIS ^{14}C AMS French INSU project, and the Region Pays de Loire program (Rising Star project TANDEM). S.T. was funded by French National Research Agency (ANR) via the LabexMER program (ANR-10-LABX-19-01) and the PIA TANDEM project (ANR-11-RSNR-00023-01). Salary and research support for the PhD student (First author) were provided by the French Ministry of Higher Education and Research. We thank S. Le Houedec for core sampling, and L. Rossignol and S. Zaragosi (University of Bordeaux) for planktonic foraminifera counting, respectively. Finally, the authors warmly acknowledge J.-F. Bourillet (Ifremer), P.I. of the BOBGEO cruise (doi.org/10.17600/9030060), for his strong support on this research project

8. References

Allen, K.A., Hönisch, B., Eggins, S.M., Haynes, L.L., Rosenthal, Y., Yu, J., 2016. Trace element proxies for surface ocean conditions: A synthesis of culture calibrations with planktic foraminifera. Geochimica et Cosmochimica Acta 193, 197–221. https://doi.org/10.1016/j.gca.2016.08.015

Altenbach AV, Pflaumann U, Schiebel R et al. 1999. Scaling percentages and distributional patterns of benthic Foraminifera with flux rates of organic carbon. Journal of Foraminiferal Research 29: 173–185.

Alvarez-Solas, J., Robinson, A., Montoya, M., Ritz, C., 2013. Iceberg discharges of the last glacial period driven by oceanic circulation changes. PNAS 110, 16350–16354. https://doi.org/10.1073/pnas.1306622110

Auffret, G.A., Boelaert, A., Vergnaud-Grazzini, C., Müller, C., Kerbrat, R., 1996. Identification of Heinrich Layers in core KS 01 North-Eastern Atlantic (46 °N, 17 °W), implications for their origin. Marine Geology, Ice Rafting and Paleocengraphy of the Northeast Atlantic Ocean Selected papers presented at the 7th European Union of Geosciences 131, 5–20. https://doi.org/10.1016/0025-3227(95)00141-7

Auffret G, Zaragosi S, Dennielou B et al. 2002. Terrigenous fluxes at the Celtic margin during the last glacial cycle. Marine Geology 188: 79–108.

Austin, W.E.N., Evans, J.R., 2000. NE Atlantic benthic foraminifera: modern distribution patterns and palaeoecological significance. Journal of the Geological Society 157, 679–691. https://doi.org/10.1144/jgs.157.3.679

Austin, W.E.N., Hibbert, F.D., Rasmussen, S.O., Peters, C., Abbott, P.M., Bryant, C.L., 2012. The synchronization of palaeoclimatic events in the North Atlantic region during Greenland Stadial 3 (ca 27.5 to 23.3 kyr b2k). Quat. Sci. Rev. 36, 154–163. https://doi.org/10.1016/j.quascirev.2010.12.014

Barras, C., Fontanier, C., Jorissen, F., Hohenegger, J., 2010. A comparison of spatial and temporal variability of living benthic foraminiferal faunas at 550m depth in the Bay of Biscay. Micropaleontology 56, 275–295.

Bergsten, H., 1994. Recent benthic foraminifera of a transect from the North Pole to the Yermak Plateau, eastern central Arctic Ocean. Marine Geology, 4th International Conference on Paleoceanography (ICP IV) 119, 251–267. https://doi.org/10.1016/0025-3227(94)90184-8

Bernhard JM. 1992. Benthic foraminiferal distribution and biomass related to pore-water oxygen content: central California continental slope and rise. Deep Sea Research Part A. Oceanographic Research Papers 39: 585–605.

Bernhard JM, Sen Gupta BK. 2003. Foraminifera of oxygen-depleted environments. In Modern Foraminifera, Sen Gupta BK (ed). Springer Netherlands:Dordrecht; 201–216.

Berx, B., Hansen, B., Østerhus, S., Larsen, K.M., Sherwin, T., Jochumsen, K., 2013. Combining in situ measurements and altimetry to estimate volume, heat and salt transport variability through the Faroe–Shetland Channel. Ocean Science 9, 639–654. https://doi.org/10.5194/os-9-639-2013

Böhm, E., Lippold, J., Gutjahr, M., Frank, M., Blaser, P., Antz, B., Fohlmeister, J., Frank, N., Andersen, M.B., Deininger, M., 2015. Strong and deep Atlantic meridional overturning circulation during the last glacial cycle. Nature 517, 73–76. https://doi.org/10.1038/nature14059

Bond, G., Broecker, W., Johnsen, S., McManus, J., Labeyrie, L., Jouzel, J., Bonani, G., 1993. Correlations between climate records from North Atlantic sediments and Greenland ice. Nature 365, 143–147. https://doi.org/10.1038/365143a0

Boswell, S.M., Toucanne, S., Pitel-Roudaut, M., Creyts, T.T., Eynaud, F., Bayon, G., 2019. Enhanced surface melting of the Fennoscandian Ice Sheet during periods of North Atlantic cooling. Geology 47, 664–668. https://doi.org/10.1130/G46370.1

Bourillet, J.-F., 2009. BOBGEO cruise,Pourquoi pas ? R/V. https://doi.org/10.17600/9030060

Bourillet, J.-F., Lericolais, G., 2003. Morphology and Seismic Stratigraphy of the Manche Paleoriver System, Western Approaches, in: Mienert, J., Weaver, P. (Eds.), European

Margin Sediment Dynamics: Side-Scan Sonar and Seismic Images. Springer, Berlin, Heidelberg, pp. 229–232. https://doi.org/10.1007/978-3-642-55846-7_37

Bourillet JF, Reynaud JY, Baltzer A, Zaragosi S. 2003. The 'Fleuve Manche': The submarine sedimentary features from the outer shelf to the deep-sea fans. Journal of Quaternary Science 18: 261–282.

Brady, E.C., Otto-Bliesner, B.L., 2011. The role of meltwater-induced subsurface ocean warming in regulating the Atlantic meridional overturning in glacial climate simulations. Clim Dyn 37, 1517–1532. https://doi.org/10.1007/s00382-010-0925-9

Broecker, W.S., Denton, G.H., 1990. The role of ocean-atmosphere reorganizations in glacial cycles. Quaternary Science Reviews 9, 305–341. https://doi.org/10.1016/0277-3791(90)90026-7

Buckley, M.W., Marshall, J., 2016. Observations, inferences, and mechanisms of the Atlantic Meridional Overturning Circulation: A review. Reviews of Geophysics 54, 5–63. https://doi.org/10.1002/2015RG000493

Buzas, M.A., 1990. Another look at conhdence limits for species proportions. Journal of Paleontology 64, 842–843. https://doi.org/10.1017/S002233600001903X

Chen, T., Robinson, L.F., Burke, A., Southon, J., Spooner, P., Morris, P.J., Ng, H.C., 2015. Synchronous centennial abrupt events in the ocean and atmosphere during the last deglaciation. Science. https://doi.org/10.1126/science.aac6159

Clark, C.D., Hughes, A.L.C., Greenwood, S.L., Jordan, C., Sejrup, H.P., 2012. Pattern and timing of retreat of the last British-Irish Ice Sheet. Quaternary Science Reviews, Quaternary Glaciation History of Northern Europe 44, 112–146. https://doi.org/10.1016/j.quascirev.2010.07.019

Clark, M., Marsh, R., Harle, J., 2021. Weakening and warming of the European Slope Current since the late 1990s attributed to basin-scale density changes (preprint). Shelf-sea depth/Data Assimilation/Shelf Seas/Transports/cycling (nutrients, C, O, etc.)/Ocean-shelf interactions. https://doi.org/10.5194/os-2021-60

Corliss BH. 1991. Morphology and microhabitat preferences of benthic foraminifera from the northwest Atlantic Ocean. Marine Micropaleontology 17: 195–236.

Corliss BH, Emerson S. 1990. Distribution of rose bengal stained deepsea benthic foraminifera from the Nova Scotian continental margin and Gulf of Maine. Deep Sea Research Part A. Oceanographic Research Papers 37: 381–400.

Crocker, A.J., Chalk, T.B., Bailey, I., Spencer, M.R., Gutjahr, M., Foster, G.L., Wilson, P.A., 2016. Geochemical response of the mid-depth Northeast Atlantic Ocean to freshwater input during Heinrich events 1 to 4. Quaternary Science Reviews 151, 236–254. https://doi.org/10.1016/j.quascirev.2016.08.035

Darling, K.F., Schweizer, M., Knudsen, K.L., Evans, K.M., Bird, C., Roberts, A., Filipsson, H.L., Kim, J.-H., Gudmundsson, G., Wade, C.M., Sayer, M.D.J., Austin, W.E.N.,

2016. The genetic diversity, phylogeography and morphology of Elphidiidae (Foraminifera) in the Northeast Atlantic. Marine Micropaleontology 129, 1–23. https://doi.org/10.1016/j.marmicro.2016.09.001

De Rijk, S., Jorissen, F.J., Rohling, E.J., Troelstra, S.R., 2000. Organic flux control on bathymetric zonation of Mediterranean benthic foraminifera. Marine Micropaleontology 40, 151–166. https://doi.org/10.1016/S0377-8398(00)00037-2

de Stigter HC 1996. Recent and fossil benthic foraminifera in the Adriatic Sea: distribution patterns in relation to organic carbon flux and oxygen concentration at the seabed. Faculteit Aardwetenschappen.

de Stigter HC, Jorissen FJ, van der Zwaan GJ. 1998. Bathymetric distribution and microhabitat partitioning of live (Rose Bengal stained) benthic Foraminifera along a shelf to bathyal transect in the southern Adriatic Sea. Journal of Foraminiferal Research 28: 40–65.

Denton, G., Anderson, R., Toggweiler, J.R., Edwards, R., Schaefer, J., Putnam, A., 2010. The Last Glacial Termination. Science (New York, N.Y.) 328, 1652–6. https://doi.org/10.1126/science.1184119

Denton, G.H., Putnam, A.E., Russell, J.L., Barrell, D.J.A., Schaefer, J.M., Kaplan, M.R., Strand, P.D., 2021. The Zealandia Switch: Ice age climate shifts viewed from Southern Hemisphere moraines. Quaternary Science Reviews 257, 106771. https://doi.org/10.1016/j.quascirev.2020.106771

Dickson, R.R., Brown, J., 1994. The production of North Atlantic Deep Water: Sources, rates, and pathways. Journal of Geophysical Research: Oceans 99, 12319–12341. https://doi.org/10.1029/94JC00530

Dorst S, Schönfeld J. 2013. Diversity of benthic foraminifera on the shelf and slope of the NE Atlantic: analysis of Datasets. Journal of Foraminiferal Research 43: 238–254.

Dorst S, Schönfeld J, Walter L. 2015. Recent benthic foraminiferal assemblages from the Celtic Sea (South Western Approaches, NE. Atlantic). Paläontologische Zeitschrift 89: 287–302.

Duros, P., Fontanier, C., de Stigter, H.C., Cesbron, F., Metzger, E., Jorissen, F.J., 2012. Live and dead benthic foraminiferal faunas from Whittard Canyon (NE Atlantic): Focus on taphonomic processes and paleo-environmental applications. Marine Micropaleontology 94–95, 25–44. https://doi.org/10.1016/j.marmicro.2012.05.004

Duros, P., Fontanier, C., Metzger, E., Pusceddu, A., Cesbron, F., de Stigter, H.C., Bianchelli, S., Danovaro, R., Jorissen, F.J., 2011. Live (stained) benthic foraminifera in the Whittard Canyon, Celtic margin (NE Atlantic). Deep Sea Research Part I: Oceanographic Research Papers 58, 128–146. https://doi.org/10.1016/j.dsr.2010.11.008

Duros P, Silva Jacinto R, Dennielou B et al. 2017. Benthic foraminiferal response to sedimentary disturbance in the Capbreton canyon (Bay of Biscay, NE Atlantic). Deep Sea Research Part I: Oceanographic Research Papers 120: 61–75.

Eynaud, F., Malaizé, B., Zaragosi, S., Vernal, A. de, Scourse, J., Pujol, C., Cortijo, E., Grousset, F.E., Penaud, A., Toucanne, S., Turon, J.-L., Auffret, G., 2012. New constraints on European glacial freshwater releases to the North Atlantic Ocean. Geophysical Research Letters 39. https://doi.org/10.1029/2012GL052100

Fatela, F., Taborda, R., 2002. Confidence limits of species proportions in microfossil assemblages. Marine Micropaleontology 45, 169–174. https://doi.org/10.1016/S0377-8398(02)00021-X

Fontanier, Christophe, Jorissen, F., Anschutz, P., Chaillou, G., 2006. Seasonal variability of benthic foraminiferal faunas at 1000 m depth in the Bay of Biscay. Journal of Foraminiferal Research 36, 61–76. https://doi.org/10.2113/36.1.61

Fontanier C, Jorissen FJ, Chaillou G et al. 2005. Live foraminiferal faunas from a 2800m deep lower canyon station from the Bay of Biscay: Faunal response to focusing of refractory organic matter. Deep Sea Research Part I: Oceanographic Research Papers 52: 1189–1227.

Fontanier, C., Jorissen, F.J., Chaillou, G., David, C., Anschutz, P., Lafon, V., 2003. Seasonal and interannual variability of benthic foraminiferal faunas at 550m depth in the Bay of Biscay. Deep Sea Research Part I: Oceanographic Research Papers 50, 457–494. https://doi.org/10.1016/S0967-0637(02)00167-X

Fontanier, C., Jorissen, F.J., Licari, L., Alexandre, A., Anschutz, P., Carbonel, P., 2002. Live benthic foraminiferal faunas from the Bay of Biscay: faunal density, composition, and microhabitats. Deep Sea Research Part I: Oceanographic Research Papers 49, 751–785. https://doi.org/10.1016/S0967-0637(01)00078-4

Fontanier C, Jorissen FJ, Michel E et al. 2008. Stable oxygen and carbon isotopes of live (stained) benthic foraminifera from cap-ferret canyon (bay of biscay). Journal of Foraminiferal Research 38: 39–51.

Fossile, E., Nardelli, M.P., Jouini, A., Lansard, B., Pusceddu, A., Moccia, D., Michel, E., Péron, O., Howa, H., Mojtahid, M., 2020. Benthic foraminifera as tracers of brine production in the Storfjorden "sea ice factory." Biogeosciences 17, 1933–1953. https://doi.org/10.5194/bg-17-1933-2020

Friocourt, Y., Levier, B., Speich, S., Blanke, B., Drijfhout, S.S., 2007. A regional numerical ocean model of the circulation in the Bay of Biscay. Journal of Geophysical Research: Oceans 112. https://doi.org/10.1029/2006JC003935

Garcia J, Mojtahid M, Howa H et al. 2013. Benthic and Planktic Foraminifera as Indicators of Late Glacial to Holocene Paleoclimatic Changes in a Marginal Environment: An Example from the Southeastern Bay of Biscay. Acta Protozoologica 52: 161–180.

Gooday, A.J., 2003. Benthic foraminifera (protista) as tools in deep-water palaeoceanography: Environmental influences on faunal characteristics, in: Advances in Marine Biology. Academic Press, pp. 1–90. https://doi.org/10.1016/S0065-2881(03)46002-1

673 Gooday, A.J., Hughes, J.A., 2002. Foraminifera associated with phytodetritus deposits
674 at a bathyal site in the northern Rockall Trough (NE Atlantic): seasonal contrasts and a
675 comparison of stained and dead assemblages. Marine Micropaleontology 46, 83–110.
676 https://doi.org/10.1016/S0377-8398(02)00050-6

677 Grousset FE, Pujol C, Labeyrie L et al. 2000. Were the North Atlantic Heinrich events
678 triggered by the behavior of the European ice sheets? Geology 28: 123–126.

679 Gupta AK. 1999. Latest Pliocene through Holocene paleoceanography of the eastern
680 Indian Ocean: benthic foraminiferal evidence. Marine Geology 161: 63–73.

681 Hammer, O., Harper, D.A.T., Ryan, P.D., 2001. PAST: Paleontological Statistics
682 Software Package for Education and Data Analysis 9.

683 Hansen, A., Knudsen, K.L., 1995. Recent foraminiferal distribution in Freemansundet
684 and Early Holocene stratigraphy on Edgeøya, Svalbard. Polar Research 14, 215–238.
685 https://doi.org/10.3402/polar.v14i2.6664

686 Hayek, L.-A., Buzas, M., 1997. Surveying Natural Populations: Quantitative Tools for
687 Assessing Biodiversity, Surveying Natural Populations. Columbia University Press.
688 https://doi.org/10.7312/haye14620

689 Hemming, S.R., 2004. Heinrich events: Massive late Pleistocene detritus layers of the
690 North Atlantic and their global climate imprint. Reviews of Geophysics 42.
691 https://doi.org/10.1029/2003RG000128

692 Henry, L.G., McManus, J.F., Curry, W.B., Roberts, N.L., Piotrowski, A.M., Keigwin,
693 L.D., 2016. North Atlantic ocean circulation and abrupt climate change during the last
694 glaciation. Science 353, 470–474. https://doi.org/10.1126/science.aaf5529

695 Herguera, J.C., Berger, W.H., 1991. Paleoproductivity from benthic foraminifera
696 abundance: Glacial to postglacial change in the west-equatorial Pacific. Geology 19, 1173–
697 1176. https://doi.org/10.1130/0091-7613(1991)019<1173:PFBFAG>2.3.CO;2

698 Hess S, Jorissen FJ. 2009. Distribution patterns of living benthic foraminifera from Cap
699 Breton canyon, Bay of Biscay: Faunal response to sediment instability. Deep Sea Research Part
700 I: Oceanographic Research Papers 56: 1555–1578.

701 Hess S, Jorissen FJ, Venet V et al. 2005. Benthic Foraminiferal recovery after recent
702 turbidite deposition in Cap Breton Canyon, Bay of Biscay. Journal of Foraminiferal Research
703 35: 114–129.

704 Huthnance, J.M., 1984. Slope Currents and "JEBAR." Journal of Physical
705 Oceanography 14, 795–810. https://doi.org/10.1175/1520-
706 0485(1984)014<0795:SCA>2.0.CO;2

707 Huthnance, J.M., Inall, M.E., Fraser, N.J., 2020. Oceanic Density/Pressure Gradients
708 and Slope Currents. Journal of Physical Oceanography 50, 1643–1654.
709 https://doi.org/10.1175/JPO-D-19-0134.1

Jennings, A.E., Weiner, N.J., Helgadottir, G., Andrews, J.T., 2004. Modern foraminiferal faunas of the southwestern to northern Iceland Shelf: oceanographic and environmental controls. Journal of Foraminiferal Research 34, 180–207. https://doi.org/10.2113/34.3.180

Jones R, Brady H. 1994. The challenger foraminifera. Oxford University Press

Jorissen FJ. 1987. The distribution of benthic foraminifera in the Adriatic Sea. Marine Micropaleontology 12: 21–48.

Jorissen FJ. 1999. Benthic foraminiferal microhabitats below the sediment-water interface. In Modern Foraminifera, Sen Gupta BK (ed). Springer Netherlands: Dordrecht; 161–179.

Jorissen FJ, Wittling I, Peypouquet JP et al. 1998. Live benthic foraminiferal faunas off Cape Blanc, NW-Africa: Community structure and microhabitats. Deep Sea Research Part I: Oceanographic Research Papers 45: 2157–2188.

Jorissen, F.J., Fontanier, C., Thomas, E., 2007. Chapter Seven Paleoceanographical Proxies Based on Deep-Sea Benthic Foraminiferal Assemblage Characteristics, in: Hillaire–Marcel, C., De Vernal, A. (Eds.), Developments in Marine Geology, Proxies in Late Cenozoic Paleoceanography. Elsevier, pp. 263–325. https://doi.org/10.1016/S1572-5480(07)01012-3

Keffer, T., Martinson, D.G., Corliss, B.H., 1988. The Position of the Gulf Stream During Quaternary Glaciations. Science 241, 440–442. https://doi.org/10.1126/science.241.4864.440

Keul, N., Langer, G., Thoms, S., de Nooijer, L.J., Reichart, G.-J., Bijma, J., 2017. Exploring foraminiferal Sr/Ca as a new carbonate system proxy. Geochimica et Cosmochimica Acta 202, 374–386. https://doi.org/10.1016/j.gca.2016.11.022

Kissel, C., Laj, C., Piotrowski, A.M., Goldstein, S.L., Hemming, S.R., 2008. Millennial-scale propagation of Atlantic deep waters to the glacial Southern Ocean. Paleoceanography 23. https://doi.org/10.1029/2008PA001624

Koho, K.A., Piña-Ochoa, E., Geslin, E., Risgaard-Petersen, N., 2011. Vertical migration, nitrate uptake and denitrification: survival mechanisms of foraminifers (Globobulimina turgida) under low oxygen conditions. FEMS Microbiology Ecology 75, 273–283. https://doi.org/10.1111/j.1574-6941.2010.01010.x

Korsun, S.A., Pogodina, I.A., Forman, S.L., Lubinski, D.J., 1995. Recent foraminifera in glaciomarine sediments from three arctic fjords of Novaja Zemlja and Svalbard. Polar Research 14, 15–32. https://doi.org/10.3402/polar.v14i1.6648

Lebreiro SM, Antón L, Reguera MI et al. 2018. Paleoceanographic and climatic implications of a new Mediterranean Outflow branch in the southern Gulf of Cadiz. Quaternary Science Reviews 197: 92–111.

Löfverström, M., Caballero, R., Nilsson, J., Kleman, J., 2014. Evolution of the large-scale atmospheric circulation in response to changing ice sheets over the last glacial cycle. Climate of the Past 10, 1453–1471. https://doi.org/10.5194/cp-10-1453-2014

748 Lozier, M.S., Li, F., Bacon, S., Bahr, F., Bower, A.S., Cunningham, S.A., Jong, M.F.
749 de, Steur, L. de, deYoung, B., Fischer, J., Gary, S.F., Greenan, B.J.W., Holliday, N.P., Houk,
750 A., Houpert, L., Inall, M.E., Johns, W.E., Johnson, H.L., Johnson, C., Karstensen, J., Koman,
751 G., Bras, I.A.L., Lin, X., Mackay, N., Marshall, D.P., Mercier, H., Oltmanns, M., Pickart, R.S.,
752 Ramsey, A.L., Rayner, D., Straneo, F., Thierry, V., Torres, D.J., Williams, R.G., Wilson, C.,
753 Yang, J., Yashayaev, I., Zhao, J., 2019. A sea change in our view of overturning in the subpolar
754 North Atlantic. Science 363, 516–521. https://doi.org/10.1126/science.aau6592

755 Lynch-Stieglitz, J., 2017. The Atlantic Meridional Overturning Circulation and Abrupt
756 Climate Change. Annu. Rev. Mar. Sci. 9, 83–104. https://doi.org/10.1146/annurev-marine-
757 010816-060415

758 Lynch-Stieglitz, J., Adkins, J.F., Curry, W.B., Dokken, T., Hall, I.R., Herguera, J.C.,
759 Hirschi, J.J.-M., Ivanova, E.V., Kissel, C., Marchal, O., Marchitto, T.M., McCave, I.N.,
760 McManus, J.F., Mulitza, S., Ninnemann, U., Peeters, F., Yu, E.-F., Zahn, R., 2007. Atlantic
761 Meridional Overturning Circulation During the Last Glacial Maximum. Science 316, 66–69.
762 https://doi.org/10.1126/science.1137127

763 Mackensen, A., Sejrup, H.P., Jansen, E., 1985. The distribution of living benthic
764 foraminifera on the continental slope and rise off southwest Norway. Marine
765 Micropaleontology 9, 275–306. https://doi.org/10.1016/0377-8398(85)90001-5

766 Marcott, S.A., Clark, P.U., Padman, L., Klinkhammer, G.P., Springer, S.R., Liu, Z.,
767 Otto-Bliesner, B.L., Carlson, A.E., Ungerer, A., Padman, J., He, F., Cheng, J., Schmittner, A.,
768 2011. Ice-shelf collapse from subsurface warming as a trigger for Heinrich events. Proc. Natl.
769 Acad. Sci. U.S.A. 108, 13415–13419. https://doi.org/10.1073/pnas.1104772108

770 Margreth, S., Rüggeberg, A., Spezzaferri, S., 2009. Benthic foraminifera as bioindicator
771 for cold-water coral reef ecosystems along the Irish margin. Deep Sea Research Part I:
772 Oceanographic Research Papers 56, 2216–2234. https://doi.org/10.1016/j.dsr.2009.07.009

773 Marsh, R., Haigh, I.D., Cunningham, S.A., Inall, M.E., Porter, M., Moat, B.I., 2017.
774 Large-scale forcing of the European Slope Current and associated inflows to the North Sea.
775 Ocean Sci. 13. https://doi.org/10.5194/os-13-315-2017

776 McCave, I.N., Manighetti, B., Beveridge, N. a. S., 1995. Circulation in the glacial North
777 Atlantic inferred from grain-size measurements. Nature 374, 149–152.
778 https://doi.org/10.1038/374149a0

779 McManus, J.F., Oppo, D.W., Cullen, J.L., 1999. A 0.5-Million-Year Record of
780 Millennial-Scale Climate Variability in the North Atlantic. Science 283, 971–975.
781 https://doi.org/10.1126/science.283.5404.971

782 McManus JF, Francois R, Gherardi J-M et al. 2004. Collapse and rapid resumption of
783 Atlantic meridional circulation linked to deglacial climate changes. Nature 428: 834–837.

784 Mendes I, Dias JA, Schönfeld J et al. 2012. Distribution of living benthic foraminifera
785 on the northern gulf of Cadiz continental shelf. Journal of Foraminiferal Research 42: 18–38.

Ménot, G., Bard, E., Rostek, F., Weijers, J.W.H., Hopmans, E.C., Schouten, S., Damsté, J.S.S., 2006. Early Reactivation of European Rivers During the Last Deglaciation. Science 313, 1623–1625. https://doi.org/10.1126/science.1130511

Milker Y, Schmiedl G. 2012. A taxonomic guide to modern benthic shelf foraminifera of the western Mediterranean Sea. Palaeontologica Electronica 15: 1–134.

Mix AC, Bard E, Schneider R. 2001. Environmental processes of the ice age: land, oceans, glaciers (EPILOG). Quaternary Science Reviews 20: 627–657.

Mojtahid M, Jorissen F, Lansard B et al. 2009. Spatial distribution of live benthic foraminifera in the Rhône prodelta: Faunal response to a continental–marine organic matter gradient. Marine Micropaleontology 70: 177–200.

Mojtahid, M., Griveaud, C., Fontanier, C., Anschutz, P., Jorissen, F.J., 2010. Live benthic foraminiferal faunas along a bathymetrical transect (140–4800m) in the Bay of Biscay (NE Atlantic). Revue de Micropaléontologie, Foraminiferal Geobiology 53, 139–162. https://doi.org/10.1016/j.revmic.2010.01.002

Mojtahid, M., Jorissen, F.J., Garcia, J., Schiebel, R., Michel, E., Eynaud, F., Gillet, H., Cremer, M., Diz Ferreiro, P., Siccha, M., Howa, H., 2013. High resolution Holocene record in the southeastern Bay of Biscay: Global versus regional climate signals. Palaeogeography, Palaeoclimatology, Palaeoecology 377, 28–44. https://doi.org/10.1016/j.palaeo.2013.03.004

Mojtahid, M., Geslin, E., Coynel, A., Gorse, L., Vella, C., Davranche, A., Zozzolo, L., Blanchet, L., Bénéteau, E., Maillet, G., 2016. Spatial distribution of living (Rose Bengal stained) benthic foraminifera in the Loire estuary (western France). Journal of Sea Research, Recent and past sedimentary, biogeochemical and benthic ecosystem evolution of the Loire Estuary (Western France) 118, 1–16. https://doi.org/10.1016/j.seares.2016.02.003

Mojtahid, M., Toucanne, S., Fentimen, R., Barras, C., Le Houedec, S., Soulet, G., Bourillet, J.-F., Michel, E., 2017. Changes in northeast Atlantic hydrology during Termination 1: Insights from Celtic margin's benthic foraminifera. Quaternary Science Reviews 175, 45–59. https://doi.org/10.1016/j.quascirev.2017.09.003

Morigi C, Jorissen FJ, Gervais A et al. 2001. Benthic foraminiferal faunas in surface sediments off nw africa: relationship with organic flux to the ocean floor. Journal of Foraminiferal Research 31: 350–368.

Moritz, M., Jochumsen, K., Kieke, D., Klein, B., Klein, H., Köllner, M., Rhein, M., 2021. Volume Transport Time Series and Variability of the North Atlantic Eastern Boundary Current at Goban Spur. Journal of Geophysical Research: Oceans 126, e2021JC017393. https://doi.org/10.1029/2021JC017393

Murray JW. 1970. Foraminifers of the Western Approaches to the English Channel. Micropaleontology 16: 471–485.

Murray, J.W., 2006. Ecology and Applications of Benthic Foraminifera. Cambridge University Press.

Murray, J.W., 2014. Ecology and Palaeoecology of Benthic Foraminifera. Routledge.

Ng HC, Robinson LF, McManus JF et al. 2018. Coherent deglacial changes in western Atlantic Ocean circulation. Nature Communications 9: 2947.

Otto-Bliesner, B.L., Brady, E.C., Clauzet, G., Tomas, R., Levis, S., Kothavala, Z., 2006. Last Glacial Maximum and Holocene Climate in CCSM3. Journal of Climate 19, 2526–2544. https://doi.org/10.1175/JCLI3748.1

Pascual, A., Rodriguez-Lazaro, J., Martín-Rubio, M., Jouanneau, J.-M., Weber, O., 2008. A survey of the benthic microfauna (foraminifera, Ostracoda) on the Basque shelf, southern Bay of Biscay. Journal of Marine Systems, Oceanography of the Bay of Biscay 72, 35–63. https://doi.org/10.1016/j.jmarsys.2007.05.015

Pascual, A., Rodríguez-Lázaro, J., Martínez-García, B., Varela, Z., 2020. Palaeoceanographic and palaeoclimatic changes during the last 37,000 years detected in the SE Bay of Biscay based on benthic foraminifera. Quaternary International, Quaternary Research in Spain: Environmental Changes and Human Footprint 566–567, 323–336. https://doi.org/10.1016/j.quaint.2020.03.043

Peck, V.L., Hall, I.R., Zahn, R., Elderfield, H., Grousset, F., Hemming, S.R., Scourse, J.D., 2006. High resolution evidence for linkages between NW European ice sheet instability and Atlantic Meridional Overturning Circulation. Earth and Planetary Science Letters 243, 476–488. https://doi.org/10.1016/j.epsl.2005.12.023

Peck, V.L., Hall, I.R., Zahn, R., Grousset, F., Hemming, S.R., Scourse, J.D., 2007. The relationship of Heinrich events and their European precursors over the past 60ka BP: a multi-proxy ice-rafted debris provenance study in the North East Atlantic. Quaternary Science Reviews 26, 862–875. https://doi.org/10.1016/j.quascirev.2006.12.002

Phleger FB, Parker FL, Peirson JF. 1953. North Atlantic foraminifera. Reports of the Swedish Deep-Sea Expedition 7: 1–122

Pina-Ochoa, E., Hogslund, S., Geslin, E., Cedhagen, T., Revsbech, N.P., Nielsen, L.P., Schweizer, M., Jorissen, F., Rysgaard, S., Risgaard-Petersen, N., 2010. Widespread occurrence of nitrate storage and denitrification among Foraminifera and Gromiida. Proceedings of the National Academy of Sciences 107, 1148–1153. https://doi.org/10.1073/pnas.0908440107

Pingree, R.D., Cann, B.L., 1990. Structure, strength and seasonality of the slope currents in the Bay of Biscay region. Journal of the Marine Biological Association of the United Kingdom 70, 857–885. https://doi.org/10.1017/S0025315400059117

Pingree, R.D., Sinha, B., Griffiths, C.R., 1999. Seasonality of the European slope current (Goban Spur) and ocean margin exchange. Continental Shelf Research 19, 929–975. https://doi.org/10.1016/S0278-4343(98)00116-2

Pollard, R.T., Pu, S., 1985. Structure and circulation of the Upper Atlantic Ocean northeast of the Azores. Progress in Oceanography 14, 443–462. https://doi.org/10.1016/0079-6611(85)90022-9

Polyak, L., Korsun, S., Febo, L.A., Stanovoy, V., Khusid, T., Hald, M., Paulsen, B.E., Lubinski, D.J., 2002. Benthic foraminiferal assemblages from the southern Kara Sea, a river-influenced Arctic marine environment. Journal of Foraminiferal Research 32, 252–273. https://doi.org/10.2113/32.3.252

Pujos, M., 1976. Ecologie des foraminifères benthiques et des thecamoebiens de la Gironde et du plateau continental Sud-Gascogne: application à la connaissance du quaternaire terminal de la région Ouest-Gironde (Thèse de doctorat). Université Bordeaux-I, 1971-2013, France.

Rasmussen, S.O., Andersen, K.K., Svensson, A.M., Steffensen, J.P., Vinther, B.M., Clausen, H.B., Siggaard-Andersen, M.-L., Johnsen, S.J., Larsen, L.B., Dahl-Jensen, D., Bigler, M., Röthlisberger, R., Fischer, H., Goto-Azuma, K., Hansson, M.E., Ruth, U., 2006. A new Greenland ice core chronology for the last glacial termination. Journal of Geophysical Research: Atmospheres 111. https://doi.org/10.1029/2005JD006079

Rasmussen SO, Seierstad IK, Andersen KK et al. 2008. Synchronization of the NGRIP, GRIP, and GISP2 ice cores across MIS 2 and palaeoclimatic implications. Quaternary Science Reviews 27: 18–28.

Rasmussen, S.O., Bigler, M., Blockley, S.P., Blunier, T., Buchardt, S.L., Clausen, H.B., Cvijanovic, I., Dahl-Jensen, D., Johnsen, S.J., Fischer, H., Gkinis, V., Guillevic, M., Hoek, W.Z., Lowe, J.J., Pedro, J.B., Popp, T., Seierstad, I.K., Steffensen, J.P., Svensson, A.M., Vallelonga, P., Vinther, B.M., Walker, M.J.C., Wheatley, J.J., Winstrup, M., 2014. A stratigraphic framework for abrupt climatic changes during the Last Glacial period based on three synchronized Greenland ice-core records: refining and extending the INTIMATE event stratigraphy. Quaternary Science Reviews, Dating, Synthesis, and Interpretation of Palaeoclimatic Records and Model-data Integration: Advances of the INTIMATE project(INTegration of Ice core, Marine and TErrestrial records, COST Action ES0907) 106, 14–28. https://doi.org/10.1016/j.quascirev.2014.09.007

Reimer PJ, Austin WEN, Bard E et al. 2020. The IntCal20 Northern Hemisphere Radiocarbon Age Calibration Curve (0–55 cal kBP). Radiocarbon 62: 725–757.

Rickaby, R.E.M., Elderfield, H., 2005. Evidence from the high-latitude North Atlantic for variations in Antarctic Intermediate water flow during the last deglaciation. Geochemistry, Geophysics, Geosystems 6. https://doi.org/10.1029/2004GC000858

Risgaard-Petersen, N., Langezaal, A.M., Ingvardsen, S., Schmid, M.C., Jetten, M.S.M., Op den Camp, H.J.M., Derksen, J.W.M., Piña-Ochoa, E., Eriksson, S.P., Peter Nielsen, L., Peter Revsbech, N., Cedhagen, T., van der Zwaan, G.J., 2006. Evidence for complete denitrification in a benthic foraminifer. Nature 443, 93–96. https://doi.org/10.1038/nature05070

Rodriguez-Lazaro, J., Pascual, A., Cacho, I., Varela, Z., Pena, L.D., 2017. Deep-sea benthic response to rapid climatic oscillations of the last glacial cycle in the SE Bay of Biscay. Journal of Sea Research, Changing Ecosystems in the Bay of Biscay: Natural and Anthropogenic Effects 130, 49–72. https://doi.org/10.1016/j.seares.2017.06.002

Rogerson, M., Rohling, E.J., Bigg, G.R., Ramirez, J., 2012. Paleoceanography of the Atlantic-Mediterranean exchange: Overview and first quantitative assessment of climatic forcing. Reviews of Geophysics 50. https://doi.org/10.1029/2011RG000376

Rühlemann, C., Mulitza, S., Lohmann, G., Paul, A., Prange, M., Wefer, G., 2004. Intermediate depth warming in the tropical Atlantic related to weakened thermohaline circulation: Combining paleoclimate data and modeling results for the last deglaciation. Paleoceanography 19. https://doi.org/10.1029/2003PA000948

Schmiedl G, Mackensen A. 1997. Late Quaternary paleoproductivity and deep water circulation in the eastern South Atlantic Ocean: Evidence from benthic foraminifera. Palaeogeography, Palaeoclimatology, Palaeoecology 130: 43–80.

Schmiedl, G., Mackensen, A., Müller, P.J., 1997. Recent benthic foraminifera from the eastern South Atlantic Ocean: Dependence on food supply and water masses. Marine Micropaleontology 32, 249–287. https://doi.org/10.1016/S0377-8398(97)00023-6

Schmiedl, G., de Bovée, F., Buscail, R., Charrière, B., Hemleben, C., Medernach, L., Picon, P., 2000. Trophic control of benthic foraminiferal abundance and microhabitat in the bathyal Gulf of Lions, western Mediterranean Sea. Marine Micropaleontology 40, 167–188. https://doi.org/10.1016/S0377-8398(00)00038-4

Schmiedl G, Mitschele A, Beck S et al. 2003. Benthic foraminiferal record of ecosystem variability in the eastern Mediterranean Sea during times of sapropel S5 and S6 deposition. Palaeogeography, Palaeoclimatology, Palaeoecology 190: 139–164.

Schönfeld, J., 1997. The impact of the Mediterranean Outflow Water (MOW) on benthic foraminiferal assemblages and surface sediments at the southern Portuguese continental margin. Marine Micropaleontology 29, 211–236. https://doi.org/10.1016/S0377-8398(96)00050-3

Schönfeld, J., 2002a. A new benthic foraminiferal proxy for near-bottom current velocities in the Gulf of Cadiz, northeastern Atlantic Ocean. Deep Sea Research Part I: Oceanographic Research Papers 49, 1853–1875. https://doi.org/10.1016/S0967-0637(02)00088-2

Schönfeld, J., 2002b. Recent benthic foraminiferal assemblages in deep high-energy environments from the Gulf of Cadiz (Spain). Marine Micropaleontology 44, 141–162. https://doi.org/10.1016/S0377-8398(01)00039-1

Schönfeld J. 2006. Taxonomy and distribution of the Uvigerina peregrina plexus in the tropical to northeastern Atlantic. Journal of Foraminiferal Research 36: 355–367.

Schönfeld, J., Altenbach, A.V., 2005. Late Glacial to Recent distribution pattern of deep-water Uvigerina species in the north-eastern Atlantic. Marine Micropaleontology 57, 1–24. https://doi.org/10.1016/j.marmicro.2005.05.004

Schroder-Adams, C., Cole, F., Medioli, F., Mudie, P., Scott, D., Dobbin, L., 1990. Recent Arctic shelf Foraminifera: seasonally ice covered vs. perennially ice covered areas.

939 Journal of Foraminiferal Research - J FORAMIN RES 20, 8–36.
940 https://doi.org/10.2113/gsjfr.20.1.8

941 Scourse, J.D., Haapaniemi, A.I., Colmenero-Hidalgo, E., Peck, V.L., Hall, I.R., Austin,
942 W.E.N., Knutz, P.C., Zahn, R., 2009. Growth, dynamics and deglaciation of the last British–
943 Irish ice sheet: the deep-sea ice-rafted detritus record. Quaternary Science Reviews 28, 3066–
944 3084. https://doi.org/10.1016/j.quascirev.2009.08.009

945 Shaffer, G., Olsen, S.M., Bjerrum, C.J., 2004. Ocean subsurface warming as a
946 mechanism for coupling Dansgaard-Oeschger climate cycles and ice-rafting events. Geophys.
947 Res. Lett. 31, L24202. https://doi.org/10.1029/2004GL020968

948 Spezzaferri, S., Rüggeberg, A., Stalder, C., Margreth, S., 2014. Taxonomic notes and
949 illustrations of benthic foraminifera from cold-water coral ecosystems. Cushman Foundation
950 Special Publication 49–140.

951 Thornalley DJR, Elderfield H, McCave IN. 2010. Intermediate and deep water
952 paleoceanography of the northern North Atlantic over the past 21,000 years. Paleoceanography
953 25: PA1211.

954 Thornalley, D.J.R., Bauch, H.A., Gebbie, G., Guo, W., Ziegler, M., Bernasconi, S.M.,
955 Barker, S., Skinner, L.C., Yu, J., 2015. A warm and poorly ventilated deep Arctic
956 Mediterranean during the last glacial period. Science 349, 706–710.
957 https://doi.org/10.1126/science.aaa9554

958 Toucanne, S., Zaragosi, S., Bourillet, J.F., Naughton, F., Cremer, M., Eynaud, F.,
959 Dennielou, B., 2008. Activity of the turbidite levees of the Celtic–Armorican margin (Bay of
960 Biscay) during the last 30,000 years: Imprints of the last European deglaciation and Heinrich
961 events. Marine Geology 247, 84–103. https://doi.org/10.1016/j.margeo.2007.08.006

962 Toucanne, S., Zaragosi, S., Bourillet, J.F., Cremer, M., Eynaud, F., Van Vliet-Lanoë,
963 B., Penaud, A., Fontanier, C., Turon, J.L., Cortijo, E., Gibbard, P.L., 2009. Timing of massive
964 'Fleuve Manche' discharges over the last 350kyr: insights into the European ice-sheet
965 oscillations and the European drainage network from MIS 10 to 2. Quaternary Science Reviews
966 28, 1238–1256. https://doi.org/10.1016/j.quascirev.2009.01.006

967 Toucanne, S., Zaragosi, S., Bourillet, J.-F., Marieu, V., Cremer, M., Kageyama, M., Van
968 Vliet-Lanoë, B., Eynaud, F., Turon, J.-L., Gibbard, P.L., 2010. The first estimation of Fleuve
969 Manche palaeoriver discharge during the last deglaciation: Evidence for Fennoscandian ice
970 sheet meltwater flow in the English Channel ca 20–18ka ago. Earth and Planetary Science
971 Letters 290, 459–473. https://doi.org/10.1016/j.epsl.2009.12.050

972 Toucanne, S., Zaragosi, S., Bourillet, J.-F., Dennielou, B., Jorry, S.J., Jouet, G., Cremer,
973 M., 2012. External controls on turbidite sedimentation on the glacially-influenced Armorican
974 margin (Bay of Biscay, western European margin). Marine Geology 303–306, 137–153.
975 https://doi.org/10.1016/j.margeo.2012.02.008

976 Toucanne, S., Soulet, G., Freslon, N., Jacinto, R.S., Dennielou, B., Zaragosi, S., Eynaud,
977 F., Bourillet, J.-F., Bayon, G., 2015. Millennial-scale fluctuations of the European Ice Sheet at

the end of the last glacial, and their potential impact on global climate. Quaternary Science Reviews 123, 113–133.

Toucanne, S., Soulet, G., Riveiros, N.V., Boswell, S.M., Dennielou, B., Waelbroeck, C., Bayon, G., Mojtahid, M., Bosq, M., Sabine, M., Zaragosi, S., Bourillet, J.-F., Mercier, H., 2021. The North Atlantic Glacial Eastern Boundary Current as a Key Driver for Ice-Sheet—Amoc Interactions and Climate Instability. Paleoceanography and Paleoclimatology 36, e2020PA004068. https://doi.org/10.1029/2020PA004068

Toucanne, S., Naughton, F., Rodrigues, T., Vázquez-Riveiros, N., Sánchez Goñi, M.F., 2022. Chapter 25 - Abrupt (or millennial or suborbital) climatic variability: Heinrich events/stadials, in: Palacios, D., Hughes, P.D., García-Ruiz, J.M., Andrés, N. (Eds.), European Glacial Landscapes. Elsevier, pp. 181–187. https://doi.org/10.1016/B978-0-12-823498-3.00062-5

van Aken, H.M., 2000. The hydrography of the mid-latitude Northeast Atlantic Ocean: II: The intermediate water masses. Deep Sea Research Part I: Oceanographic Research Papers 47, 789–824. https://doi.org/10.1016/S0967-0637(99)00112-0

Van der Zwaan GJ, Jorissen FJ. 1991. Biofacial patterns in riverinduced shelf anoxia. Geological Society, London, Special Publications 58: 65–82.

Vénec-Peyré M-T, Le Calvez Y. 1988. Les Foraminifères épiphytes de l'herbier de Posidonies de Banyuls-sur-Mer (Méditerranée occidentale): étude des variations spatio-temporelles du peuplement. Cahiers de Micropaléontologie 3: 21–40.

Waelbroeck, C., Lougheed, B.C., Vazquez Riveiros, N., Missiaen, L., Pedro, J., Dokken, T., Hajdas, I., Wacker, L., Abbott, P., Dumoulin, J.-P., Thil, F., Eynaud, F., Rossignol, L., Fersi, W., Albuquerque, A.L., Arz, H., Austin, W.E.N., Came, R., Carlson, A.E., Collins, J.A., Dennielou, B., Desprat, S., Dickson, A., Elliot, M., Farmer, C., Giraudeau, J., Gottschalk, J., Henderiks, J., Hughen, K., Jung, S., Knutz, P., Lebreiro, S., Lund, D.C., Lynch-Stieglitz, J., Malaizé, B., Marchitto, T., Martínez-Méndez, G., Mollenhauer, G., Naughton, F., Nave, S., Nürnberg, D., Oppo, D., Peck, V., Peeters, F.J.C., Penaud, A., Portilho-Ramos, R. da C., Repschläger, J., Roberts, J., Rühlemann, C., Salgueiro, E., Sanchez Goni, M.F., Schönfeld, J., Scussolini, P., Skinner, L.C., Skonieczny, C., Thornalley, D., Toucanne, S., Rooij, D.V.,

Wang, Y.J., Cheng, H., Edwards, R.L., An, Z.S., Wu, J.Y., Shen, C.-C., Dorale, J.A., 2001. A High-Resolution Absolute-Dated Late Pleistocene Monsoon Record from Hulu Cave, China. Science 294, 2345–2348. https://doi.org/10.1126/science.1064618

Wollenburg, J.E., Kuhnt, W., 2000. The response of benthic foraminifers to carbon flux and primary production in the Arctic Ocean. Marine Micropaleontology 40, 189–231. https://doi.org/10.1016/S0377-8398(00)00039-6

Wollenburg, J.E., Mackensen, A., 1998. Living benthic foraminifers from the central Arctic Ocean: faunal composition, standing stock and diversity. Marine Micropaleontology 34, 153–185. https://doi.org/10.1016/S0377-8398(98)00007-3

Wollenburg JE, Mackensen A. 2009. The ecology and distribution of benthic foraminifera at the Håkon Mosby mud volcano (SW Barents Sea slope). Deep Sea Research Part I: Oceanographic Research Papers 56: 1336–1370.

Wollenburg JE, Kuhnt W, Mackensen A. 2001. Changes in Arctic Ocean paleoproductivity and hydrography during the last 145 kyr: The benthic foraminiferal record. Paleoceanography 16: 65–77.

Wollenburg, J.E., Knies, J., Mackensen, A., 2004. High-resolution paleoproductivity fluctuations during the past 24 kyr as indicated by benthic foraminifera in the marginal Arctic Ocean. Palaeogeography, Palaeoclimatology, Palaeoecology 204, 209–238. https://doi.org/10.1016/S0031-0182(03)00726-0

Yu, J., Elderfield, H., Jin, Z., Tomascak, P., Rohling, E.J., 2014. Controls on Sr/Ca in benthic foraminifera and implications for seawater Sr/Ca during the late Pleistocene. Quaternary Science Reviews 98, 1–6. https://doi.org/10.1016/j.quascirev.2014.05.018

Zahn R, Schönfeld J, Kudrass H-R et al. 1997. Thermohaline instability in the North Atlantic during meltwater events: Stable isotope and ice-rafted detritus records from Core SO75-26KL, Portuguese Margin. Paleoceanography 12: 696–710.

Zaragosi, S., Eynaud, F., Pujol, C., Auffret, G.A., Turon, J.-L., Garlan, T., 2001. Initiation of the European deglaciation as recorded in the northwestern Bay of Biscay slope environments (Meriadzek Terrace and Trevelyan Escarpment): a multi-proxy approach. Earth and Planetary Science Letters 188, 493–507. https://doi.org/10.1016/S0012-821X(01)00332-6

Zaragosi, S., Bourillet, J.-F., Eynaud, F., Toucanne, S., Denhard, B., Van Toer, A., Lanfumey, V., 2006. The impact of the last European deglaciation on the deep-sea turbidite systems of the Celtic-Armorican margin (Bay of Biscay). Geo-Mar Lett 26, 317–329. https://doi.org/10.1007/s00367-006-0048-9

Zou, S., Lozier, S., Zenk, W., Bower, A., Johns, W., 2017. Observed and modeled pathways of the Iceland Scotland Overflow Water in the eastern North Atlantic. Progress in Oceanography 159, 211–222. https://doi.org/10.1016/j.pocean.2017.10.003

1047 **Table 1.** ^{14}C dates of core BOBGEO-CS05.

Core label	Depth (cm)	Lab. Number [a]	Species	^{14}C age (yr BP)	error (1σ)	Reservoir correction [b] (^{14}C yr)	error [b] (1σ)	^{14}C age corrected for reservoir [c] (^{14}C yr BP)	error [d] (1σ)	Calendar age range [e] (yr BP, 2σ)
BOBGEO-CS05	0	Poz-73846	*N. pachyderma*	14100	80	970	200	13130	215	15133-16357
BOBGEO-CS05	10	Poz-42911	bulk planktonic	14770	70	970	200	13800	212	16132-17333
BOBGEO-CS05	305-309	Beta-478193	*G. bulloides*	15270	40	400	200	14870	204	17550-18661
BOBGEO-CS05	446	SacA-29355	bulk planktonic	18090	60	400	200	17690	209	20890-22026
BOBGEO-CS05	500-505	Beta-478194	*G. bulloides*	17140	50	400	200	16740	206	19773-20716
BOBGEO-CS05	660	SacA-29356	bulk planktonic	21140	200	400	200	20740	283	24238-25672
BOBGEO-CS05	796-800	Beta-478195	*G. bulloides*	19680	60	400	200	19280	209	22885-23789
BOBGEO-CS05	933-935	Beta-478196	*G. bulloides*	20430	70	400	200	20030	212	23727-24665
BOBGEO-CS05	1030-1033	Beta-478197	*G. bulloides*	21830	70	400	200	21430	212	25220-26049
BOBGEO-CS05	1230	Poz-45912	bulk planktonic	24510	240	400	200	24110	312	27726-28959
BOBGEO-CS05	1350	SacA-29357	bulk planktonic	24220	100	400	200	23820	224	27624-28628
BOBGEO-CS05	1460	Poz-73848	*N. pachyderma*	26130	230	400	200	25730	305	29237-30490

a: Poz- (Poznan Radiocarbon Lab., Poland); Beta- (Beta Analytic, USA); SacA- (SMA Artemis, France)

b: Reservoir correction inferred from Stern et Lisieki (2013); see Toucanne et al. (2015) for details

c: Corrected ^{14}C ages are obtained by subtracting the reservoir correction to the original ^{14}C age

d: Errors associated to the corrected ^{14}C were propagated through the quadratic sum

e: Corrected ^{14}C ages were calibrated using the atmospheric calibration curve IntCal20 (Reimer et al., 2020)

1048

1049 **Table 2.** Taxonomic reference list, microhabitat and ecological preferences for the
1050 dominant benthic species (>5 %) and the corresponding bibliographic references.

Species	References with images	Microhabitat	Ecological preferences	Plate 1	Plate 2
Bolivina spp.		Shallow infaunal (John W. Murray, 2006)	*Bolivina* spp. have opportunistic behaviour (Schmiedl *et al.*, 2000) and ecological preferences for phytodetritus enriched deposits (Duros *et al.*, 2017, 2011)	5-6	
Cassidulina carinata Silvestri, 1896	Phleger *et al.* (1953), p1. 9, Figs. 32–37	Epifaunal to shallow infaunal (Jorissen, 1987; Altenbach *et al.*, 1999)	*Cassidulina carinata* is an opportunistic species (Fontanier et al., 2003; Duros et al., 2011) that lives in OM-enriched sediments (Hess *et al*., 2005; Hess and Jorissen, 2009).	7	
Cassidulina crassa d'Orbigny, 1839	Jorissen (1987), pl. 1, Fig. 3	Shallow infaunal (de Stigter *et al*., 1998; Fontanier et al., 2005)	In our case, *Cassidulina crassa* could be a morphospecies of *Cassidulina reniforme*. This latter is often transported from the continental shelf, and redeposited on glacial marine sediments (Mackensen *et al*., 1985), until 1000m water depth in Arctic (Wollenburg and Mackensen, 2009).	8	
Cibicides lobatulus Walker and Jacob, 1798	Jones and Brady (1994), pl. 93, Fig. 1	Epifaunal (John W. Murray, 2006)	*Cibicides lobatulus* live at shallow depth, attached on seagrass and algae (Vénec-Peyré and Le Calvez, 1988; John W. Murray, 2006). Even if, they were described as transported species, they can be found alive in deep and high energy environments (*e.g.* Schönfeld, 1997, 2002b, 2002a; Margreth *et al.*, 2009; Spezzaferri *et al.*, 2015)	13	
Cibicidoides pachyderma Rzehak, 1886	Jones and Brady (1994), pl. 94, Fig. 9	Shallow infaunal (Fontanier et al., 2003, 2002)	*Cibicidoides pachyderma* live in meso-oligotrophic conditions (Fontanier et al., 2003; Mojtahid et al., 2009). They prefer low nutrients waters (Schmiedl *et al.*, 2000).	11-12	b
Chilostomella oolina Schwager, 1878	Jones and Brady (1994), pl. 55, Fig. 12-14	Deep Infaunal (Corliss and Emerson, 1990; Bernhard, 1992; Jorissen *et al.*, 1998)	*Chilostomella oolina* is adapted to anoxic or suboxic conditions (Fontanier *et al*., 2002; Bernhard and Sen Gupta, 2003). They may be replaced by *Globobulimina* spp. when the degraded OM quality decreases (Fontanier *et al.*, 2002)	4	
Elphidium clavatum Cushman, 1930	Darling *et al.* (2016), Fig. 4, S4	Infaunal–epifaunal (John W. Murray, 2006)	*Elphidium clavatum* is a widespread taxon, mainly distributed in the Arctic, and frequent in glacier-proximal environments. It is found living down to several hundreds of meters depths in the Arctic and in the Baltic (Jennings et al., 2004; John W. Murray, 2006; Darling et al., 2016; Fossile et al., 2020). In the nearby study of Mojtahid *et al.* (2017), *Elphidium* species found at 1000 m depth during the last deglaciation were interpreted as being possibly transported from shallower settings.	10	a
Elphidium gerthi van Voorthuysen, 1957	Mendes *et al. (*2012), Fig. 4, 8		*Elphidium gerthi* is a subtidal to intertidal species, very coommon along the western European coasts . In the nearby study of Mojtahid *et al.* (2017), *Elphidium* species found at 1000 m depth during the last deglaciation were interpreted as being possibly transported from shallower settings.	9	

Species	**References with images**	**Microhabitat**	***Ecological preferences***	**Plate 1**	**Plate 2**
Globobulimina spp.		Deep infaunal (John W. Murray, 2006)	*Globobulimina* spp. live in organically-enriched and/or oxygen-depleted sediments (*e.g.* Jorissen, 1999; Schmiedl *et al.*, 2003; Mojtahid *et al.*, 2010). They can live in anoxic sediments by respiring nitrates (Risgaard-Petersen *et al.*, 2006).	3	
Gavelinopsis praegeri Heron-Allen & Earland, 1913	Jorissen (1987), pl. 3, Fig. 13	Epifaunal (Jorissen, 1987)	*Gavelinopsis praegeri is an epiphytic species living in a wide range of water depths in marine environments (John W. Murray, 2006). They are found down to 1200m water depth (de Stigter, 1996) and prefers more oxic conditions (Dorst et al., 2015).*	16	
Hoeglundina elegans d'Orbigny, 1826	Milker and Schmiedl, (2012), pl. 19, Fig. 15	Epifaunal; shallow infaunal (Jorissen et al., 1998; Fontanier et al., 2002)	*Hoeglundina elegans is described as indicator of low organic carbon environments (Fontanier et al., 2002; Morigi et al., 2001).*	17	
Nonionella turgida Williamson, 1858	Milker and Schmiedl, (2012), pl. 26, Figs. 1-5	Deep infaunal (Corliss, 1991)	*Nonionella turgida is an opportunistic species, tolerant to low oxygen conditions and high nutrient level (Van der Zwaan and Jorissen, 1991).*	2	
Planorbulina mediterranensis d'Orbigny, 1826	Jones and Brady (1994), pl. 92, Fig. 1	Epifaunal (Murray, 2006)	*Planorbulina mediterranensis is an epiphytic species and lives at shallow depths (Murray, 2006).*	15	
Pullenia quinqueloba Reuss, 1851	Jones and Brady (1994), pl. 84, Fig. 14	Intermediate infaunal (Corliss, 1991; C. Fontanier et al., 2008)	*Pullenia quinqueloba can live in low-organic carbon conditions (Gupta, 1999).*	18	
Textularia sagittula Defrance, 1824	Jorissen (1987), pl. 3, Fig. 12	Epifaunal (Murray, 2006)	*Textularia sagittula is an agglutinated species (Murray, 2006). They are dominant in shallow water depths, on sandy sediments (Murray, 2014)*	1	
Trifarina angulosa Williamson, 1858	Jones and Brady (1994), pl. 74, Fig. 15	Shallow infaunal (Hess and Jorissen, 2009)	*Trifarina angulosa have been observed in phytodetritus-enriched sediment (e.g. Hess and Jorissen, 2009; Duros et al., 2011). They are often associated with C. lobatulus to strong bottom currents and can be observed until 1000m water depth (Mackensen et al., 1985).*	14	

1051

9. Tables caption

Table 3. ^{14}C dates of core BOBGEO-CS05.

Table 4. Taxonomic reference list, microhabitat and ecological preferences for the dominant benthic species (>5 %) and the corresponding bibliographic references.

10. Figures caption

Figure 1. Location of the study area. a) 3D representation (N-S, W-E and in water depth) of the modern oceanic circulation in the North Atlantic representing the main currents (acronyms written in black), water masses (acronyms written in colors) and the Subpolar (in blue) and Subtropical (in red) gyres in the North Atlantic. b) Bathymetric map representing the paleogeographic and paleoceanographic configuration (i.e. ice sheets, the Channel River, currents, and water masses) of the North Atlantic during the Last Glacial Stadials according to Toucanne et al. (2021). The angulous shapes represent the icebergs. c) Bathymetric map focussing on the study area and showing the location of our study core BOBGEO-CS05 (violet star), together with nearby cores at 1000 m water depth (black stars): MD95-2002 (Eynaud et al., 2012; Ménot et al., 2006; Toucanne et al., 2015), MD99-2328 (Mojtahid et al., 2017), PP10-12 (Pascual et al., 2020). For the detailed description of the general modern and glacial circulation in the North Atlantic and in the study area, the reader is referred to the text (Section 2). LGM: Last Glacial Maximum.

Figure 2. Age model of core BOBGEO-CS05.a) Chronostratigraphic framework of core BOBGEO-CS05 based on the synchronisation of XRF-Ca/Ti ratios with cores MD95-2002 and MD99-2328 (Zaragosi et al., 2006; Mojtahid et al., 2017; Toucanne et al., 2021). b) Sediment Accumulation Rate (SAR; full line) and 14C dates (orange triangles) with associated errors in core BOBGEO-CS05. The 14C dates represented by empty triangles are outliers (cf. section 3.1. for further details). In red is represented the final age model based on XRF-Ca/Ti synchronisation (cf. Fig. 2a). c) Test of the robustness of the age model with the percentages of the polar planktonic species *N. pachyderma* in core BOBGEO-CS05 (this study) with core MD95-2002 (Grousset et al., 2000) and MD99-2328 (Mojtahid et al., 2017). d) NGRIP δ18O (GICCS05 chronology; Rasmussen et al., 2006, 2014). f) X-Ray photographs (cf. Supplementary material S1 for the whole core) showing the four observed facies. Blue triangles: 14C dates of core MD95-2002 (Toucanne et al., 2021); Orange and empty triangles: 14C dates

of core BOBGEO-CS05; Blue bands: Heinrich Stadials (HSs); Gray bands: Heinrich Events (HEs); Greenland Interstadial (GI); Last Glacial Maximum (LGM); Marine Isotope Stage (MIS).

Figure 3. Benthic foraminiferal data from core BOBGEO-CS05. a) Benthic Foraminiferal Accumulation Rates (BFAR; ind.cm^{-3}.ka^{-1}) for the >150 µm (full line) and the >63 µm fraction (dashed line). b) Shannon index (H). c-j) Relative abundances (%) of the eight most representative benthic foraminiferal species (>10 %). Full lines and dashed lines represent respectively the > 150 µm and >63 µm fractions. Brown lines represent data from the >150 µm fraction of core MD99-2328 (Mojtahid et al., 2017). Yellow bands: Greenland Interstadials (GI); gray bands: Heinrich Events (HEs); blues bands: Heinrich Stadial (HSs). Marine Isotope Stage (MIS). The vertical dashed grey line represents the limit between early HS1 (ca. 18.2 - 16.7 cal ka BP) and late HS1 (ca. 16.7 – 14.7 cal ka BP). To better highlight the variations of the different species groups, the scale of the ordinate axis is not constant.

Figure 4. Benthic foraminiferal response to ice-sheet/AMOC dynamics. a) Relative abundance of *N. pachyderma* in core BOBGEO-CS05. b) Relative abundances of glacier-proximal indicator species (% *Elphidium excavatum f. clavatum* + % *C. crassa*) in core BOBGEO-CS05. c) BIT-index at site MD95-2002 as a proxy for continental-derived material input (Ménot et al., 2006). d) Relative abundances of high-organic flux indicator species (% *C. carinata* + % *Bolivina* spp.) in core BOBGEO-CS05. e) Bermuda Rise $^{231}Pa/^{230}Th$ compilation as a proxy for AMOC export at >2 000 m depth (McManus et al., 2004; Böhm et al., 2015; Henry et al., 2016). f) XRF-Zr/Rb (violet line) and $\overline{SS}$ (pink line) composite records from the northeast Atlantic including BOBGEO-CS05 as proxies for the reconstruction of GEBC flow speed changes (Toucanne et al., 2021). g) Relative abundances of high-energy indicator species (% *C. lobatulus* + % *T. angulosa*) in core BOBGEO-CS05. h) Relative abundances of meso-oligotrophic indicator species (% *C. pachyderma*) in core BOBGEO-CS05. i) Relative abundances of anoxia indicator species (% *Globobulimina* spp. + % *C. oolina*). To better highlight the variations of the different species groups, the scale of the ordinate axis is not constant. The main events and climatic phases are reported similarly to Figure 3.

Figure 5. Focus on HS2. a) Relative abundances of the planktonic species N. pachyderma in core BOBGEO-CS05 (black line; this study) and MD95-2002 (blue line; Grousset et al., 2000).

b) XRF-Zr/Rb (violet line) and $\overline{SS}$ (pink line) composite records from the northeast Atlantic (including BOBGEO-CS05) as proxies for the reconstruction of GEBC flow speed changes (Toucanne et al., 2021). c) Relative abundances of high-energy indicator species (% C. lobatulus + % T. angulosa) in core BOBGEO-CS05. d) Benthic Foraminiferal Accumulation Rates (BFAR; ind.cm^{-3}.ka^{-1}) for the >150 µm in core BOBGEO-CS05. e) Relative abundances of meso-oligotrophic indicator species (% *C. pachyderma*) in core BOBGEO-CS05. f) Relative abundances of anoxia indicator species (% *Globobulimina* spp. + % *C. oolina*) in core BOBGEO-CS05. Dashed vertical line: Heinrich Event 2 (HE2) sensu stricto according to the regional Ca/Ti synchronisation (cf. Table S2 in Toucanne et al., 2021); blue bands: the HS2a,b cold events (Bard et al., 2000); yellow band: the mid-HS2 re-ventilation event. To better highlight the variations of the different species groups, the scale of the ordinate axis is not constant.

11. Plates caption

Plate 1. SEM photographs of the dominant benthic species (>5 % in at least one sample): 1) *Textularia sagittula* ; 2) *Nonionella turgida* ; 3) *Globobulimina affinis* ; 4) *Chilostomella oolina* ; 5) *Bolivina subaenariensis*; 6) *Bolivina albatrossi*; 7) *Cassidulina carinata*; 8) *Cassidulina crassa*; 9) *Elphidium gerthi* ; 10) *Elphidium excavatum* f. *clavatum* ; 11) *Cibicidoides pachyderma* ; 12) *Cibicides lobatulus*; 13) *Trifarina angulosa*; 14) *Planorbulina mediterranensis*; 15) *Gavelinopsis praegeri* ; 16) *Hoeglundina elegans* ; 17) *Pullenia quinqueloba*. Scale bar = 100µm.

Plate 2. *a)* Natural light photographs of *Elphidium excavatum f. clavatum* showing pyritised and altered shells. b) SEM photographs showing the variability of the morphotypes (in lateral view) lumped into *Cibicidoides pachyderma* in this study.

12. Supplementary materials caption

S1. X-Ray imagery of core BOBGEO-CS05

S2. Figure representing the relative abundances of taxa present between 5 and 10 % in at least one sample

S3. Raw foraminiferal counts

Figure 1

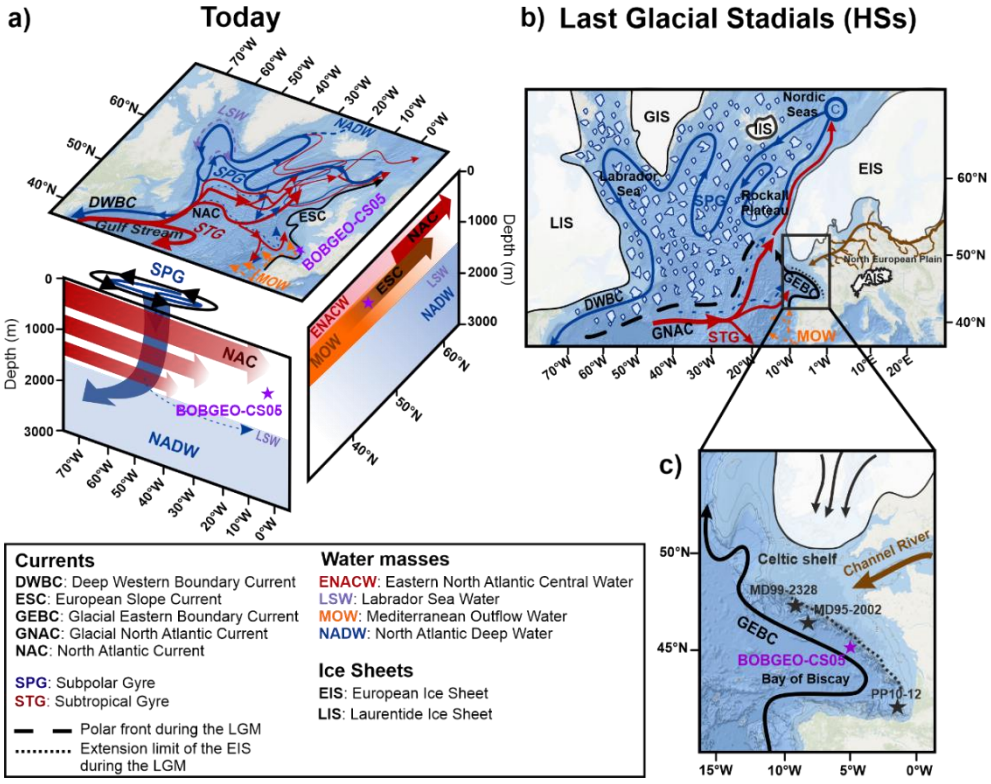
a)
Today
b) Last Glacial Stadials (HSs)
c)
DWBC
NAC
ESC
SPG
STG
MOW
LSW
NADW
BOBGEO-CS05
Gulf Stream
ENACW
GIS
LIS
EIS
Nordic Seas
Labrador Sea
Rockall Plateau
North European Plain
GNAC
GEBC
Celtic shelf
Channel River
MD99-2328
MD95-2002
Bay of Biscay
PP10-12
Depth (m)
Currents
DWBC: Deep Western Boundary Current
ESC: European Slope Current
GEBC: Glacial Eastern Boundary Current
GNAC: Glacial North Atlantic Current
NAC: North Atlantic Current
SPG: Subpolar Gyre
STG: Subtropical Gyre
Polar front during the LGM
Extension limit of the EIS during the LGM
Water masses
ENACW: Eastern North Atlantic Central Water
LSW: Labrador Sea Water
MOW: Mediterranean Outflow Water
NADW: North Atlantic Deep Water
Ice Sheets
EIS: European Ice Sheet
LIS: Laurentide Ice Sheet

Figure 2

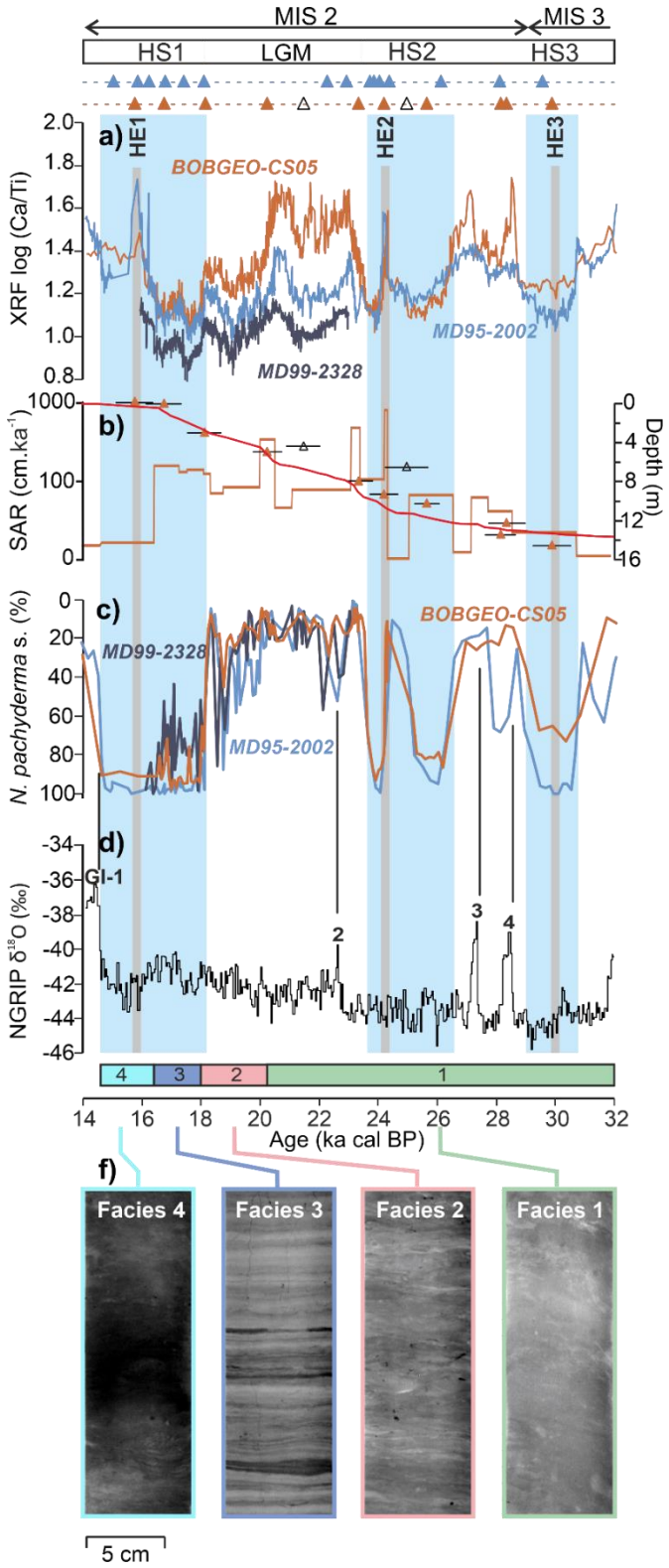
MIS 2
MIS 3
HS1
LGM
HS2
HS3
a)
HE1
HE2
HE3
BOBGEO-CS05
MD95-2002
MD99-2328
XRF log (Ca/Ti)
b)
SAR (cm.ka-1)
Depth (m)
c)
N. pachyderma s. (%)
d)
GI-1
NGRIP δ18O (‰)
4
3
2
1
Age (ka cal BP)
f)
Facies 4
Facies 3
Facies 2
Facies 1
5 cm

1162 **Figure 3**

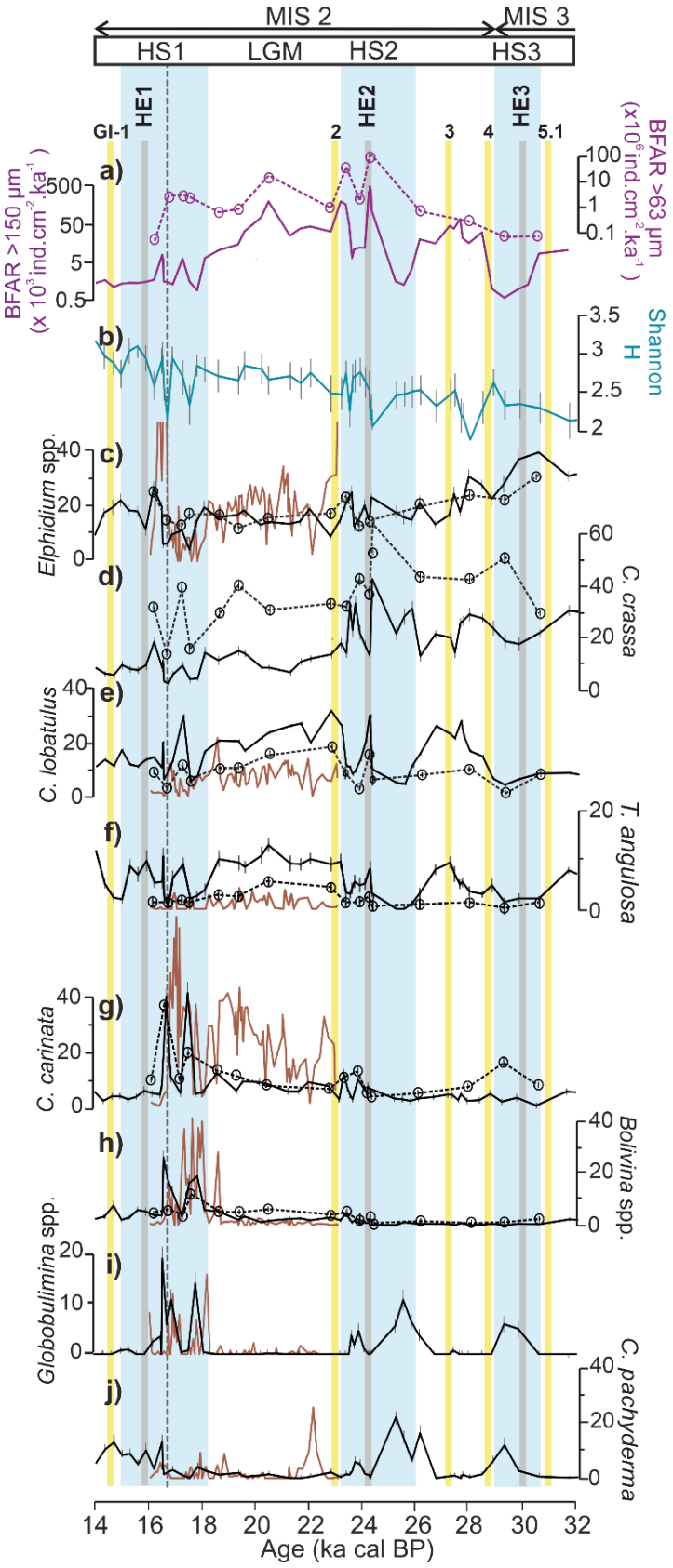

1163
1164

Figure 4

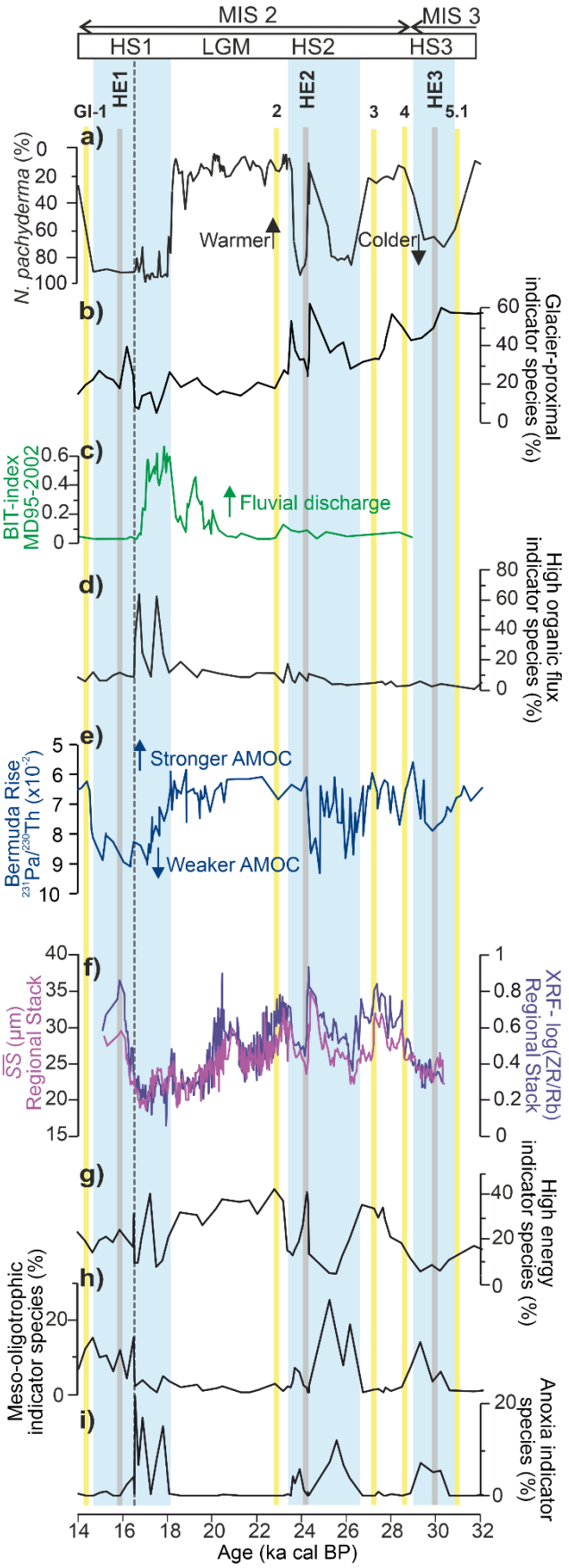
MIS 2
MIS 3
HS1
LGM
HS2
HS3
HE1
HE2
HE3
GI-1
2
3
4
5.1
a)
N. pachyderma (%)
Warmer
Colder
b)
Glacier-proximal indicator species (%)
c)
BIT-index MD95-2002
Fluvial discharge
d)
High organic flux indicator species (%)
e)
Bermuda Rise $^{231}Pa/^{230}Th$ (x10^{-2})
Stronger AMOC
Weaker AMOC
f)
$\overline{SS}$ (µm) Regional Stack
XRF- log(ZR/Rb) Regional Stack
g)
High energy indicator species (%)
h)
Meso-oligotrophic indicator species (%)
i)
Anoxia indicator species (%)
Age (ka cal BP)

Figure 5

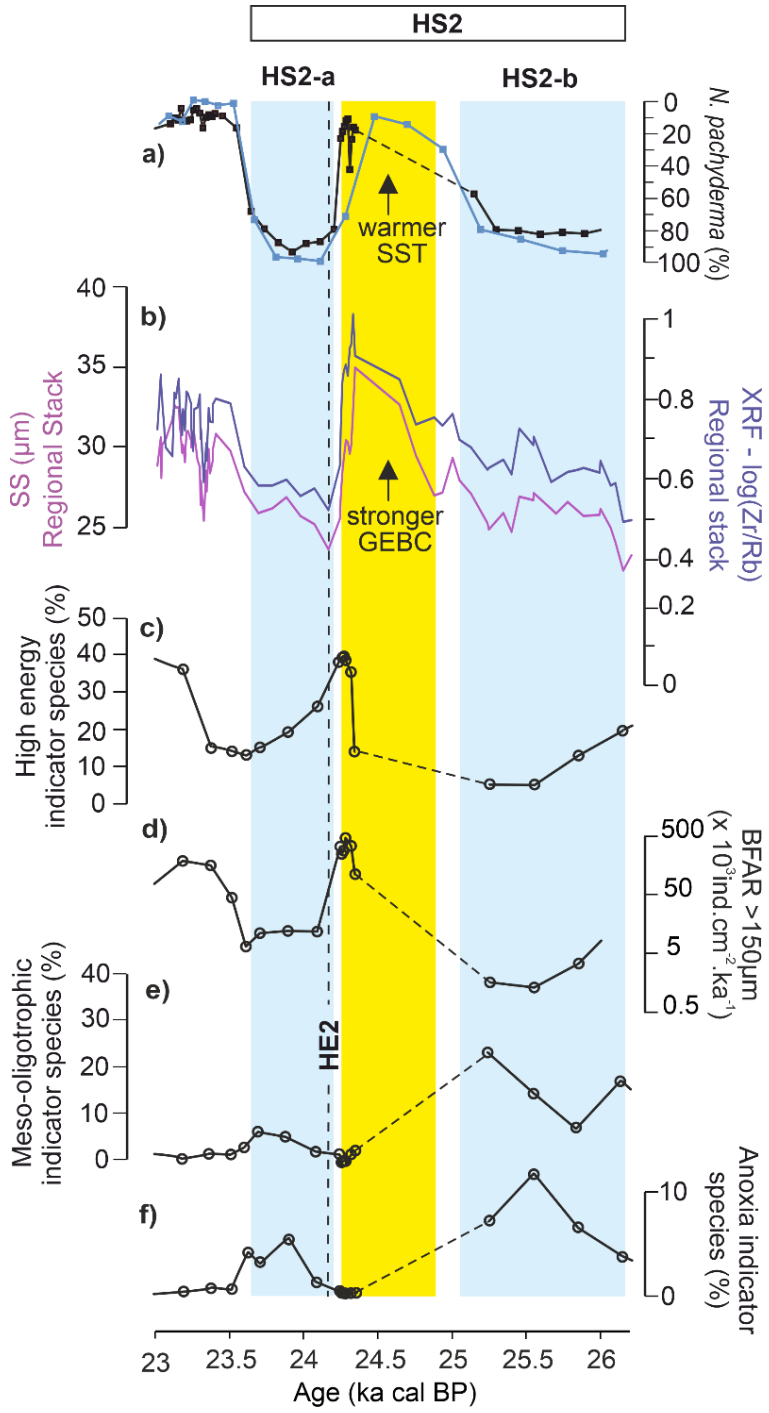
HS2
HS2-a
HS2-b
a)
warmer SST
N. pachyderma (%)
0
20
40
60
80
100
b)
stronger GEBC
SS (µm) Regional Stack
40
35
30
25
XRF - log(Zr/Rb) Regional stack
1
0.8
0.6
0.4
0.2
0
c)
High energy indicator species (%)
50
40
30
20
10
0
d)
BFAR >150µm (x 10³ind.cm⁻².ka⁻¹)
500
50
5
0.5
e)
Meso-oligotrophic indicator species (%)
40
30
20
10
0
H2
f)
Anoxia indicator species (%)
10
0
23
23.5
24
24.5
25
25.5
26
Age (ka cal BP)

Plate 1

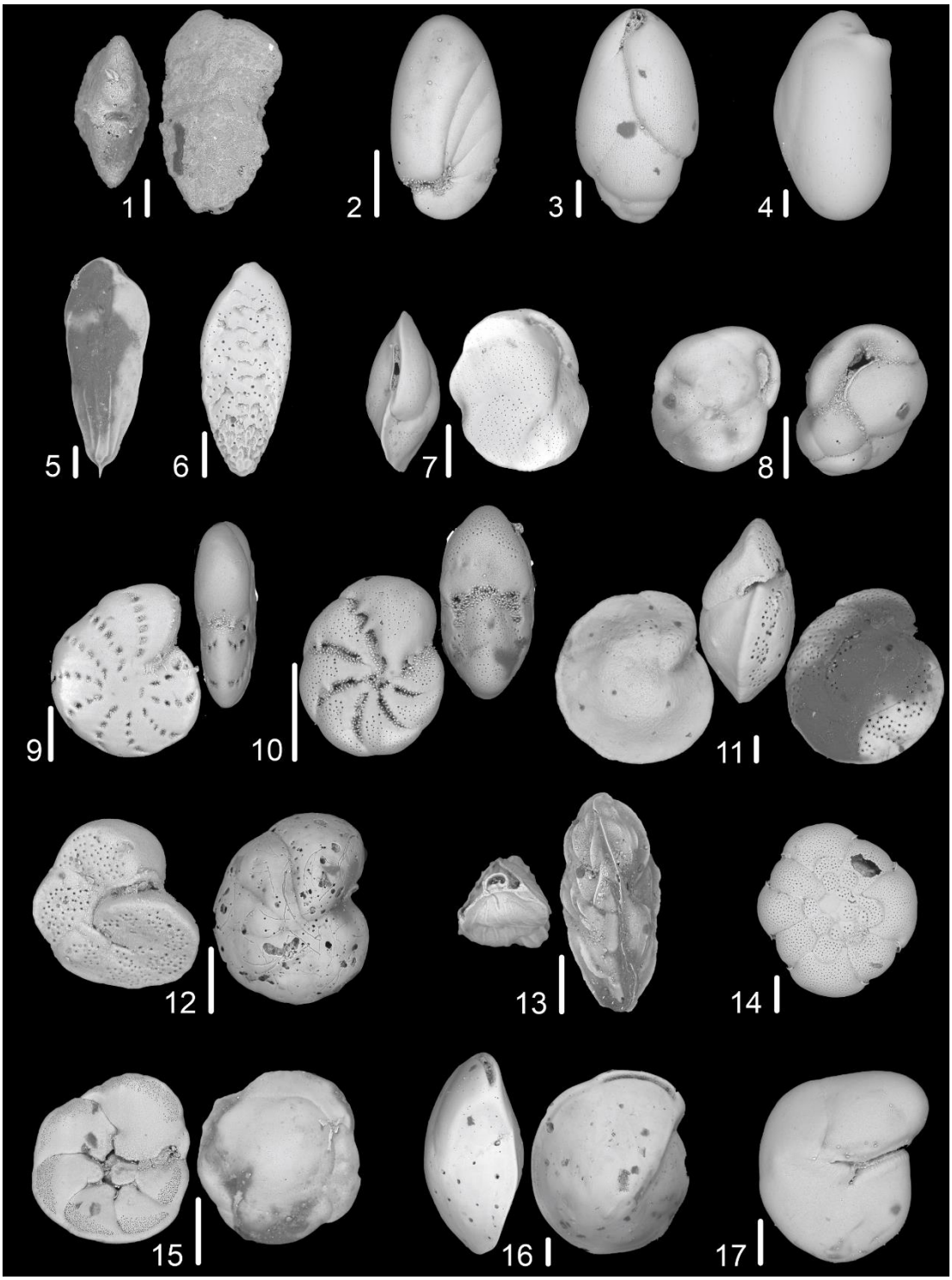

Plate 2

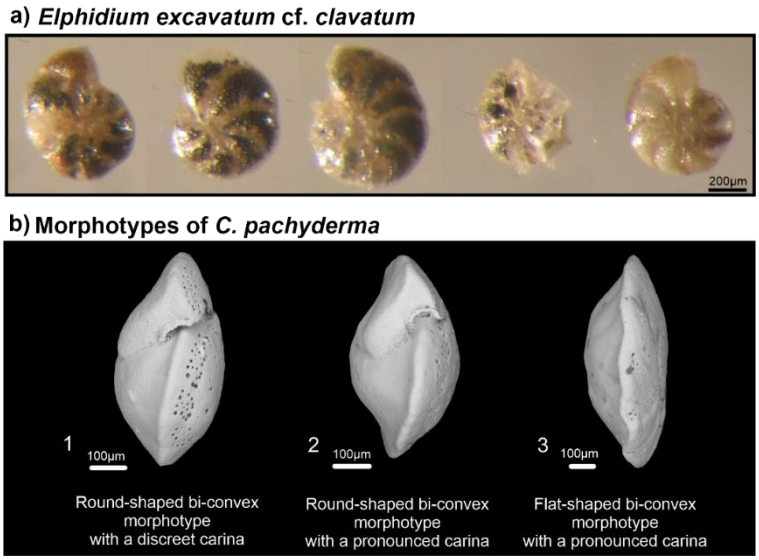
a) Elphidium excavatum cf. clavatum
200µm
b) Morphotypes of C. pachyderma
1
100µm
Round-shaped bi-convex morphotype with a discreet carina
2
100µm
Round-shaped bi-convex morphotype with a pronounced carina
3
100µm
Flat-shaped bi-convex morphotype with a pronounced carina

Supplementary material

S1

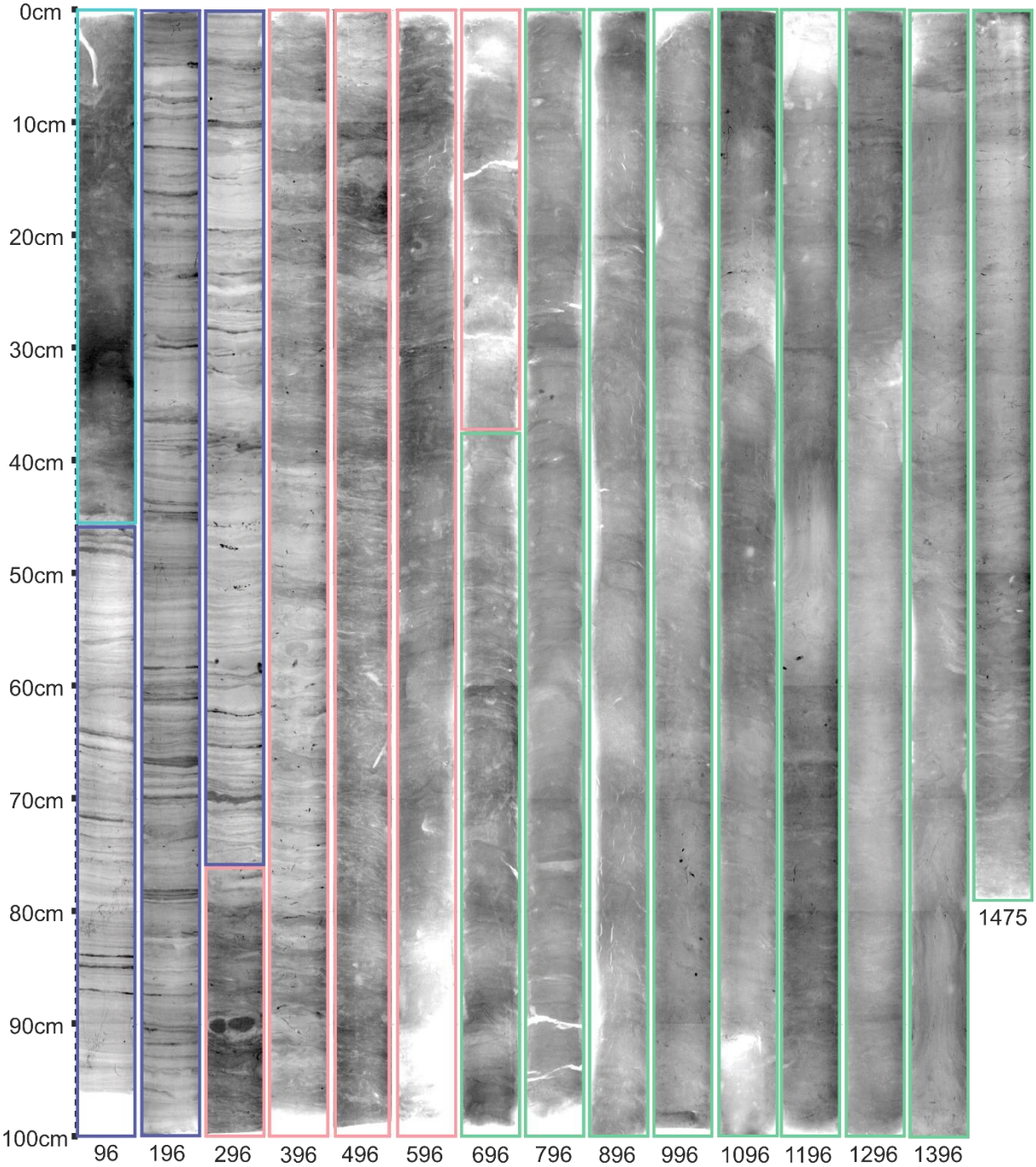

S2

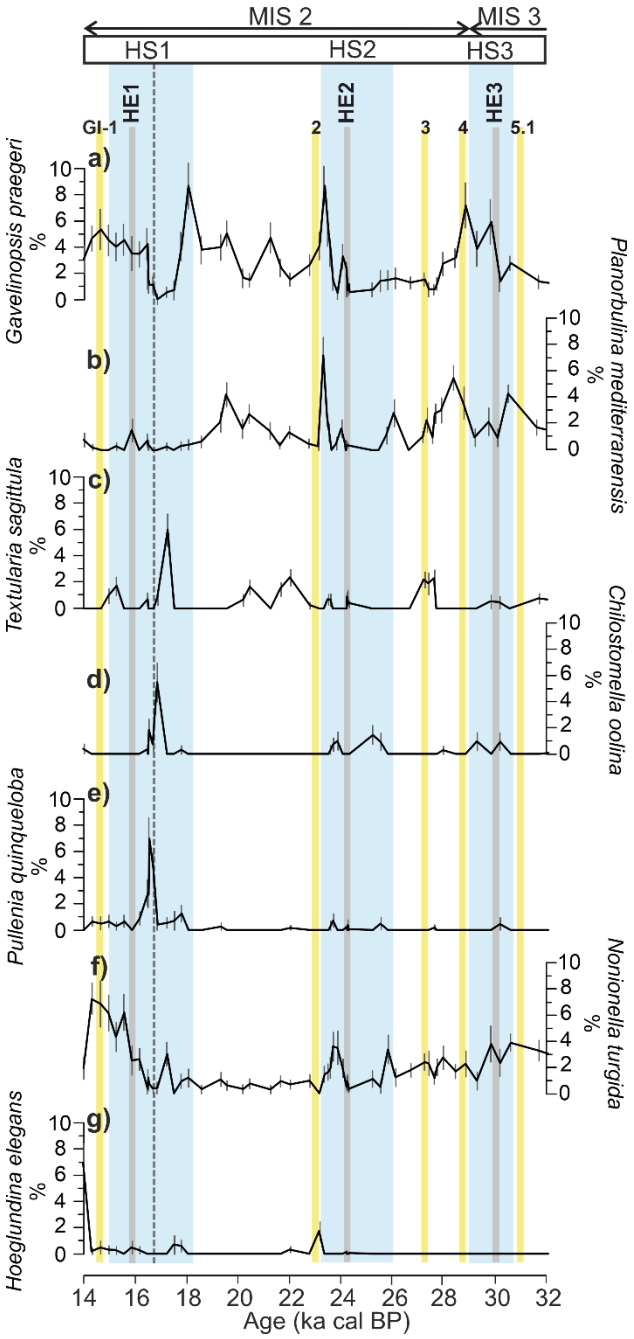

S3. Raw foraminiferal counts available in https://doi.org/10.17882/88029